ENGINEERING THE ELECTRONIC PROPERETIES OF ARMCHAIR GRAPHENE NANORIBBONS VIA Mn/Cr TERMINATION

Dissertation
Submitted in partial fulfilment of the requirements
for the degree of

MASTER OF TECHNOLOGY
in
NUCLEAR SCIENCE AND ENGINEERING(NSE)
By

Mohit Kumar Daksh
(2K13/NSE/08)

Under the guidance of

Dr. Nitin K. Puri
Asst. Prof. Department of Applied Physics
Delhi Technological University
Delhi, India

Department of Applied Physics
Delhi Technological University
(Formerly Delhi College of Engineering)
Delhi

July 2016

DELHI TECHNOLOGICAL UNIVERSITY
Established by Govt. of Delhi vide Act 6 of 2009
(*Formerly Delhi College of Engineering*)
Shahbad Daulatpur, Main Bawana Road, Delhi-110042

CERTIFICATE

This is to certify that this dissertation, entitled **Engineering the electronic properties of Armchair Graphene Nanoribbons via Mn/Cr termination**, is the authentic work carried out by **Mr. Mohit Kumar Daksh (2K13/NSE/08)** under my guidance and supervision in partial fulfillment for award of degree of **Master of Technology (M. Tech)** in **Nuclear Science and Engineering** by Department of Applied Physics in Delhi Technological University(Formerly Delhi College of Engineering), Delhi during the year 2013-2016.

As per the candidate declaration, this work has not been submitted elsewhere for the award of any other degree.

(Signature of Guide)	*(Signature of Guide)*
Dr. Nitin K. Puri	Prof. S.C Sharma (HOD)
Asst. Prof.Department of Applied Physics	Department of Applied Physics
Delhi Technological University	Delhi Technological University

DECLARATION

I, hereby, declare that the work being presented in this dissertation, entitled**Engineering the electronic properties of Armchair Graphene Nanoribbons via Mn/Cr termination,** is an authentic record of my own work carried out under the guidance of **Dr. Nitin K. Puri**, Asst. Prof. Applied Physics Department, Delhi Technological University (Formerly Delhi College of Engineering), Delhi. The work contained in this dissertation has not been submitted in part or full, to any other university or institution for award of any degree or diploma.

This dissertation is submitted to **Delhi Technological University** (Formerly Delhi College of Engineering) in partial fulfillment for the **Master of Technology (M. Tech)** in **Nuclear Science and Engineering** during the academic year 2015-2016.

_____

(Signature and Name of Student)

Mohit Kumar Daksh

(2K13/NSE/08)

ACKNOWLEDGEMENT

I take this opportunity to express my sincere gratitude to all those who have been instrumental in the successful completion of this dissertation.

Dr. Nitin K. Puri, Assistant Professor, Department of Applied Physics, Delhi Technological University (Formerly Delhi College of Engineering), Delhi, my dissertation guide,who has guided me in the successful completion of this dissertation. It is worth mentioning that he always provided me with the necessary guidance and support. Furthermore I would like to thank Dr. Neha Tyagi for introducing me to the topic as well for the immense support on the way.

I would also like to express my gratitude to my dear friend cum a wonderful roommate Vinay kumar kohli with whom I have had many insightful discussions which have cleared my understanding of various topics.

MOHIT KUMAR DAKSH

2K13/NSE/08

M.Tech (NSE)

ABSTRACT

The structural and electronics properties of Mn and Cr- terminated armchair graphene nanoribbons (AGNRs) in our present paper employing ab-initio approach based on Density Functional Theory. Maintaining self-consistency throughout the simulations, we used Local Density approximation (LDA) as proposed by Perdew and Zunger to account for the exchange and correlation energy term. Stability analysis has been done by calculating the binding energy per atom of each configuration, while electronic properties are deduced from the study of band structures and density of states. Binding energy calculations suggest that one edge Mn terminations are energetically more favorable than double edge termination. Our simulation results show that the addition of Mn and Cr impurities at the edges of AGNRs greatly enhances the stability and lowers the band gap in general .Interestingly strong hybridization is the reason due to which direct band gap of H-terminated AGNR is changed into the indirect band gag in most of the configurations. Our calculation further strengthen the argument that the transition metal as a impurity in the AGNRs can play an important role in the band gap engineering of nano ribbons for future application in the nano-semiconductor devices.

TABLE OF CONTENTS

LIST OF FIGURES

LIST OF TABLES

NOTATIONS

N_a= Width of Armchair Graphene Nanoribbon

μ = Mobility

R_H= Hall Coefficient

V_g= Gate Voltage

n= Charge Density

e= Electronic Charge

σ_{xy}= Conductivity

h= Planck's constant

E_b = Binding Energy

CHAPTER 1

INTRODUCTION

1.1 INTRODUCTION

Graphene is a single layer of one atom thickness with atoms arranged in a repeated hexagonal shape called honeycomb lattice structure. As a single carbon atom is connected with σ (sigma) bonds to its neighbouring three atoms and both above and below the graphene's plane there are Л orbitals which are partially filled, it can be termed as purely two dimension structure of carbon .It can be aptly seen as the building block of many allotropes of the carbon namely Graphite, Bucky ball and Carbon Nanotubes .Graphene are layered upon each other in graphite that are bonded through weak Van der Waal forces .Where as Carbon nanotubes are also rolled honey combed graphene sheet in cylindrical shapes and Bucky ball are wrapped rounded forms of the sheet.

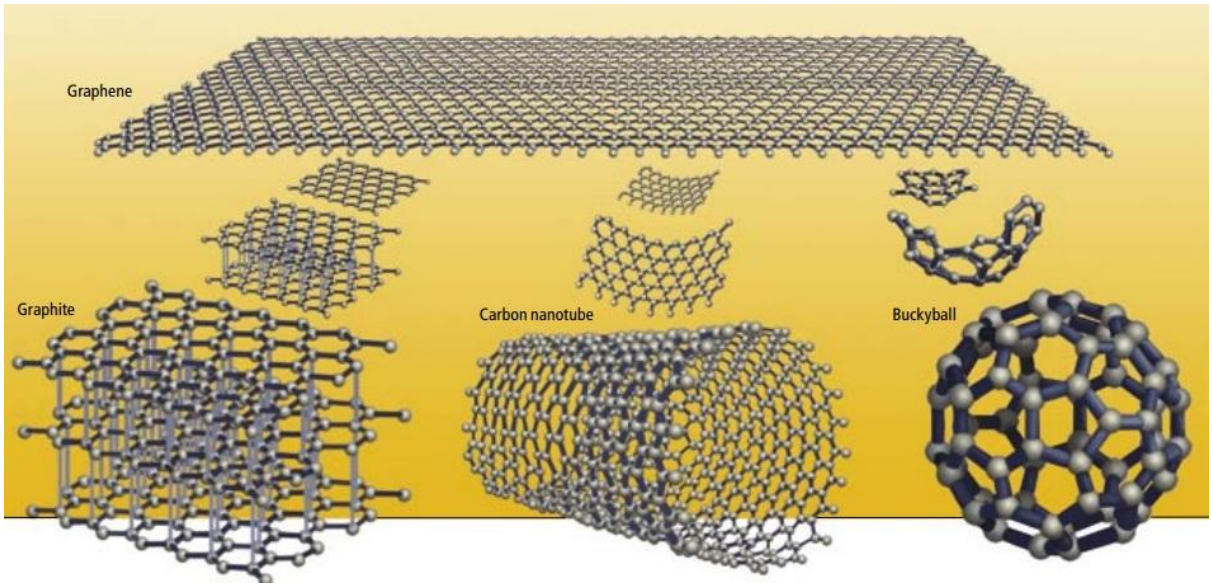

Figure 1.1 Allotropes of Carbon and their structure

Graphene is intrinsically present in many carbon forms but its free existence was always doubted upon as in normal ambient condition it was considered to be thermodynamically unstable. It was nothing less than serendipity when it was experimentally isolated first time almost a decade ago (1).The free standing sheet of carbon was termed nothing less than magical .Since then this this wonder material has taken the world of condensed matter physics by storm due to its slew of exceptional physical, structural and electronic properties .Though Graphene has been around us since a long time as it is produced when the surface of

graphite is rubbed with any other surface for example in pencils marks and other like uses but it was always hidden from our eyes. It was not until 1947 A.D. when it was theorized by P.R.Wallac during a study of properties of graphite and further described the graphene's band structure in his ground breaking paper.Many year later this was followed by the emergence of massless Dirac equation that played an important role in explaining its unusual properties. For many decades researchers tried to isolate it from graphite but they were unsuccessful .Techniques like chemical exfoliation was used in which foreign elements are inserted between the planes of graphite and they are torn apart but only things that were obtained were thinner pieces of graphite. Eventually the early interest in exfoliation technique faded away. Hence there was growing consensus among scientists that it's free existence might not be a possibility at room temperature. However in 2004 A.D. persistent efforts of scientist A. K. Geim and K. S. Novoselov bore fruits when they isolated the graphene for the first time with a relatively rudimentary technique called micro mechanical cleavage (1).They achieved success with almost a bench top apparatus in which they held a layer of graphite between two faces of folded sticky tapes and when they are unfolded it tears away some layers .Numerous iterations of the above process high crystalline quality of graphene sheets .After this for their further 'Pioneering work in Graphene' in explain its exotic properties and explaining its behaviour they were awarded the Noble Prize in Physics in 2010 A.D. Since then a spate of scientific research has begun which is aptly termed as 'THE RISE OF GRAPHENE '.

1.2 MOTIVATION FOR THE THESIS

Graphene, a hexagonal honeycomb shaped lattice of single atom thick carbon atoms was experimentally fabricated first time in 2004 and since then it has beenbuzz of the town in the condensed matter physics due to its unusual physical and chemical properties [1].Only after this Graphene gained prominence in both in theoretical as well as experimental research. It was believed that it will eventually replace silicon in nanoelectronics, spintronics and FETs with its outstanding properties such as a high speed mobility of career and a high thermal conductivity [1-4]. However in the development of commercially viable devices, the path is stilled mired with difficulties as graphene shows metallic behaviour at charge neutrality point (Dirac point) owing to its inability to electrostatically confine charges and hence has a zero band gap [5].Hence creating and maintaining the desired band gap with tuning the work function, have been major focus of the recent studies so that it can be used as a semiconductor [6-7].

One such method is to modify Graphene sheets into quasi-one dimensional structures (Q1Ds) called Graphene Nanoribbons (GNRs) creating a finite band gap in the ribbons in one configuration and other properties due to quantum confinement in AGNRs and staggered sub lattice potential which highly depends on the width (W) and chirality of the ribbon [8].There are mainly two types of nanoribbons viz. armchair-edged (AGNRs) and zigzag edged (ZGNRs) [9].Though another configuration , Klein edge has also been proposed and verified experimentally [10].AGNRs can show metallic or semiconductor behaviour depending on its width and they are also non-magnetic , whereas ZGNRs show metallic behaviour regardless of their width and exhibits magnetic properties too [8].Dangling bonds at the edges of the ribbons are very reactive and thus are usually terminated with hydrogen. This process is called edge passivation by hydrogen and resulting armchair ribbons are called hydrogen-terminated armchair graphene nanoribbons H-AGNRs. Hydrogen passivation has been extensively studied and results show that it converts indirect band gaps into direct one [7,11-12].It has been shown that edge passivation by hydrogen increases the stability and also increases the band gap further [7]. Other methods applied for band gap engineering include passivation by elements other than hydrogen including transition metals [7, 13-15] and putting uniaxial mechanical strain on the lattice [11] and twisting the graphene ribbons [16]. All methods change the band gap in one way or another and it can be said that in practical applications these effects will work together and will subsequently determine the electronic properties and band structure of the ribbon. Methods of preparation of GNRs includes single layer epitaxial grown graphene on a different substrate (Ru, SiC, Cu,) [17-19] and unzipping longitudinally nanotubes [20-21] and mechanically cutting from graphene sheet [22].Magnetic properties of Mn doped AGNRs have already been studied by Gorjizadeh and Kawazoe and they found that ribbons does not have any preference between the ferromagnetic and antiferromagnetic [23] .

We have studied the electronics and structural properties AGNRs by terminating their single edge and double edge with Mn and Cr. As AGNRs are categorized into these families namely 3m+1, 3m+2, 3m where m is an integer depending upon their widths due to their quantum confinement effects [24-25]. Maintaining consistency with the previous conventions, we have also denoted width of AGNRs as "N_a" which represents the number of C-C pairs forming the width of the ribbons. We have considered two width from each family (Na= 4 to 9) to account the width effects.

1.3 THESIS OUTLINE

This thesis aims to provide the general introduction to graphene and its exceptional properties and other related information in addition to the fundamental research work that has been carried out in it. In no way this should be taken as an exhaustive treatment of graphene properties as there are other excellent resources available forthat but I firmly believe that this can surely serve as a starting point for anybody and provide a glimpse into the wonderful world of graphene. *Chapter 1*dwells into the theoretical background associated with graphene and how it eventually came onto the big picture.In *Chapter 2 section 1* provides details about the electrical, mechanical and optical properties of graphene. *Chapter 2 section 2* elaborates into the different method of graphene synthesis and pros and cons associated with them.*Section 3* of the same chapter deals with the characterization techniques that are used to differentiate the graphene and also its types like single layer, double layer and few layer graphene. *Section 4* gives information about the potential applications and recent trends in the industries. *Chapter 3*deals with the methodology and theory used in the calculations. *Chapter 4* elaborates on the simulation results and discuss the underlying cause and effect. *Chapter 5*draws the conclusion from the results and discussion and also discuss the future scope of the work.

CHAPTER 2

GRAPHENE

2.1 STRUCTURE AND PROPERTIES

Graphene is a single layer atomic structure that resembles a honeycomb assembly. The qualitative analysis was first time done by P. R. Wallace decades ago and had been only used to explain the other allotropes of carbon and there properties. As graphite is made up of hundreds of layers of graphene whereas nanotubes are rolled sheets single layer of atoms. The structure can be viewed as two interpenetrating sub lattice of triangular shape as shown in figure 2below and explained using tight binding approach using nearest neighbour hopping. Every carbon atom in the lattice has three bonds namely one s and two p_x and p_y while p_z is out of the lattice plane forming valence and conduction and valence bands with the neighbouring atom's p_z orbital. This unique structure is responsible for its exceptional electronics and mechanical properties.

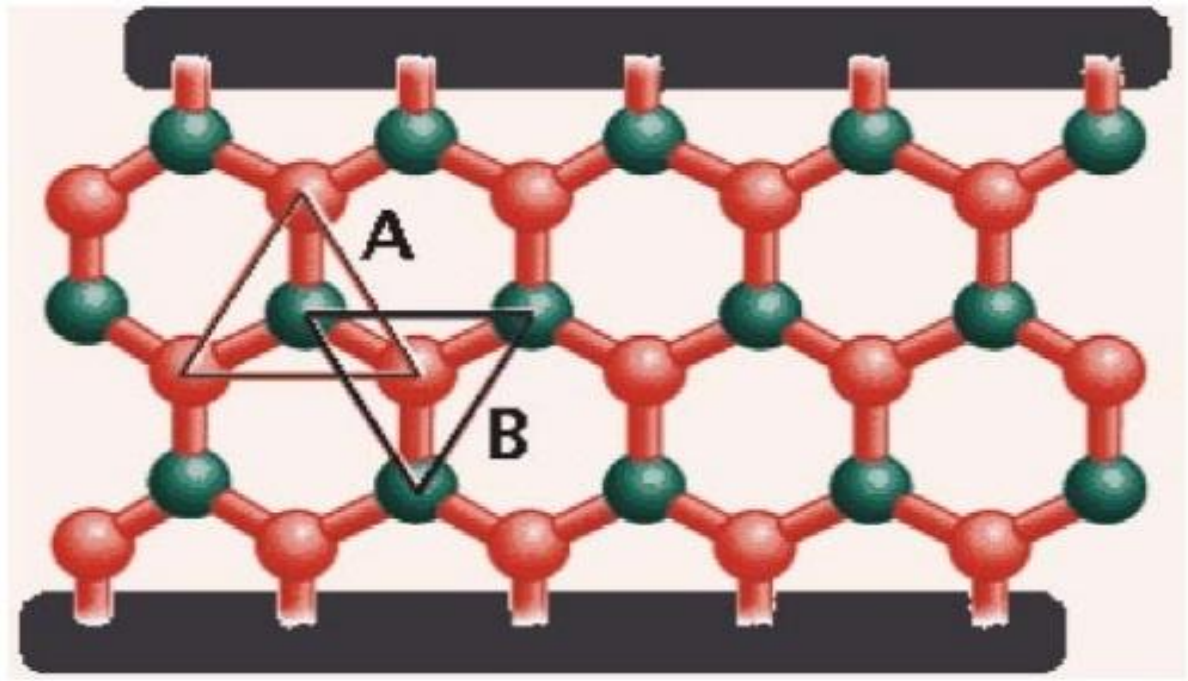

Figure 2.1 Graphene lattice showing unit cell containing two atoms A and B[26]

One of the exceptional feature it exhibits is the highly crystalline quality it exhibits despite the relatively simple methods from which it is prepared. Researchers have so far failed to find any atomic vacancy at any site or any out of the plan deformation when it is prepared from mechanical exfoliation technique. This perfect crystalline pattern is the result of the strong inter-atomic bonding between the carbon atoms. The same can be used to explain the large amount of the mechanical strain that it can sustain before getting permanently deformed. Moreover the quality of electrical conductance is directly proportional to the crystal lattice quality. Electrons can travel a long distance without being scattered off and without any impediment giving rise to high electrical conductivity. Electronics also behave differently in graphene from the electronics in ordinary metallic conductor. As the electric field is applied between the metal negatively charged electrons move towards the positive electrode. They travel a free mean path before colliding with other electrons. These charge carrier are called quasi particles which travel with a speed much slower than the speed of light in the conducting metal eliminating the need of any relativistic correction. Their interaction with conductor can be easily explained by the newton's classic mechanics or non-relativistic quantum mechanics. The two and fro motion of electrons give them an effective mass. This is where the whole scenario changes in graphene. The electrons in graphene interact with benzene like structure and give rise to a completely different type of quasi particle behaviour that can't be described by ordinary relativistic quantum mechanics. Transport of electrons in graphene is governed by the relativistic Dirac's equation .This wonderful two dimension system allows experiment in a simple bench top apparatus giving access to rich and subtle quantum electrodynamics physics. In graphene the conduction and valence band meet at the six point and two of the point are called K and K$^{'}$ as shown in figure 2.2. The Fermi lies exactly at the meeting point making graphene a zero band gap semiconductor or semi metal. Theses point are called charge neutrality or Dirac point. Near theses point the dispersion relation comes out to be linear whereas it is parabolic for conductor though graphene has very high measured conductivity. Dirac points are so called because Dirac equation is used to describe the behaviour of charge particles contrary to expectation Schrodinger equation can't be used here though it widely describe the transport in condensed matter world. Consequently the electrons behaves like the relativistic particles with zero effective mass due to their interaction with benzene like structure of carbon atoms. This all made graphene to exhibits completely different electronic properties

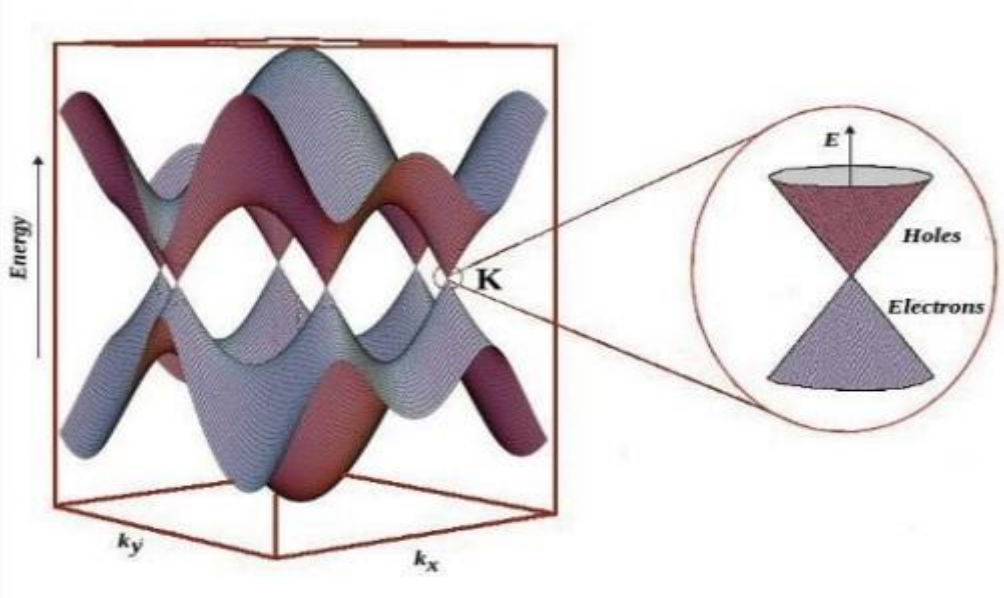

Figure 2.2 Linear energy dispersion relation of graphene and meeting of conduction and valence band at Dirac cone[26]

Graphene's exceptional electrical properties are evident in its ambipolar electric field where mobility μ of both electrons and holes were measured in excess of 15000 $cm^2\ V^{-1}\ s^{-1}$ even at room temperature [27].This mobility transport into ballistic transport on submicron scale (up to ≈0.3 μm at 300K [27].Where both charge carriers can be easily tuned even at very high concentration η as high as $10^{13}\ cm^{-2}$ .More interestingly graphene's charge mobility has weak dependency on temperature and is mostly limited only by lattice defect and scattering by impurities. Figure 4 and 5 show electric effect in graphene. Conduction σ increases with increase in voltage for both electrons and holes and charge carrier changes at gate voltage V_g sign .Hall coefficient $R_H=1/ne$ varies as $1/V_g$ where e is electronic charge and n is holes or electron concentration .This shows that there are no trapped charges in graphene and all induced carriers are mobile .

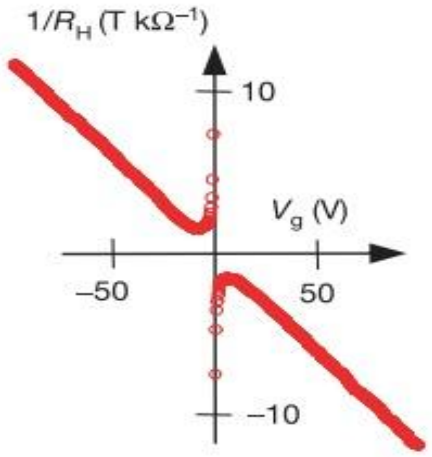

Figure 2.3 Changes in graphene's hall coefficient R_H as a function of gate voltage Vg[1]

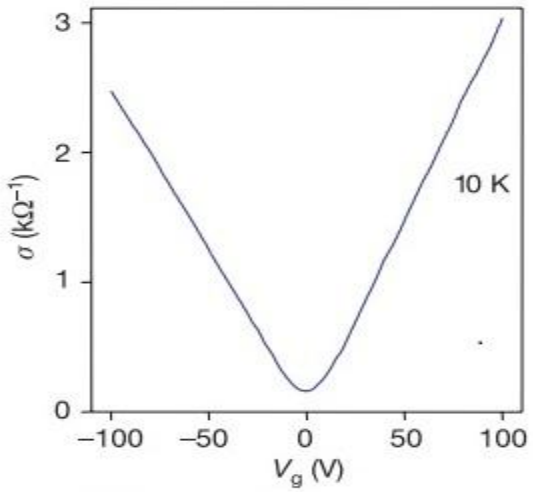

Figure 2.4Changes in graphene's conductivity σ as a function of gate voltage V[1]

Due to response of massless electron to magnetic field graphene shows a very unusual quantum hall effect. Figure 2.5shows Hall conductivity σ_{xy}plotted as a function of hole and electron in constant magnetic field **B.** Contrary to the expectations the plateaux in QHE didn't occur at the expected sequence of $\sigma_{xy} = (4e^2/h)N$ where N is integer but occurs at sequence of $(4e^2/h)(N+1/2)$.This culminated into ladder that contains equidistant steps that goes uninterrupted when passing from zero as evident in figure. This behaviour gains more importance when it find out that sequence return to former one in two layer graphene indicating electron gain a net mass in two layer graphene.

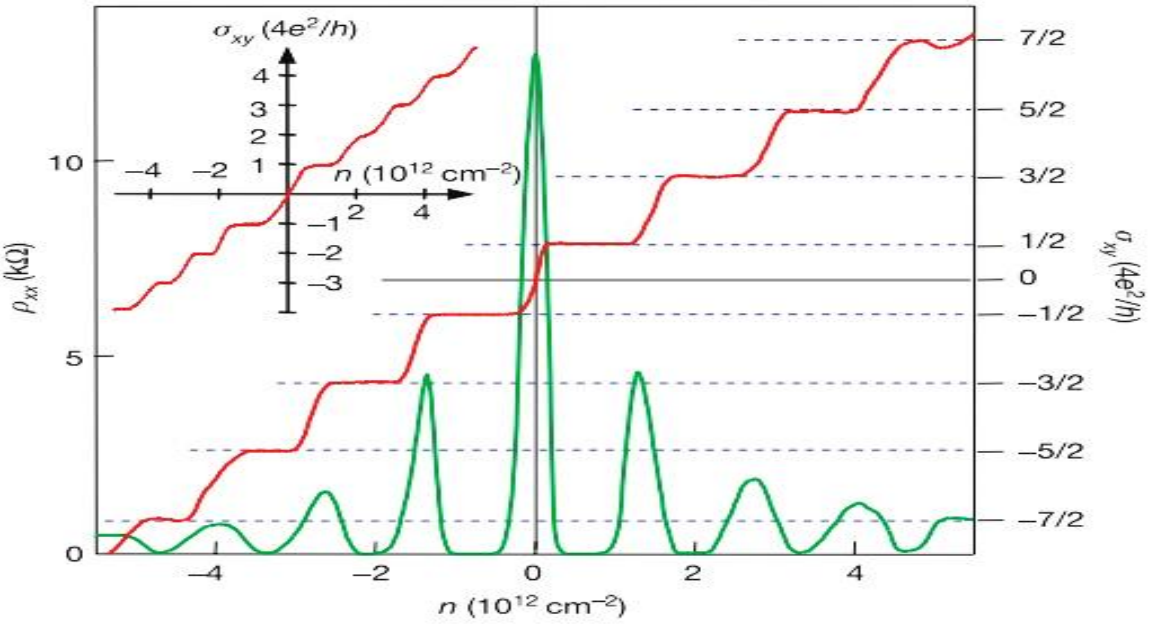

Figure 2.5QHE for massless Dirac fermions. Hall conductivity σ_{xy} andlongitudinal resistivity ρ_{xx} graphene as a function of their concentrationat B ¼ 14 T and T ¼ 4 K[1].

Graphene reflected 97.7% of incident light, only absorbing 2.3% of it despite just being a single layer of carbon atoms [28].Every layer added increase the ability to absorb more light. Optical properties can be manipulated by modifying Fermi energy level by applying gate voltage and this has been used to try to develop IR emitter, modulators and detectors[29] .Graphene is also made luminescent by opening a band gap by modifying into nanoribbons and quantum dots .combined exceptional and electrical and optical properties has made graphene a promising candidate in the field for future application of touch screens, light emitting diodes, transparent and optical limitersHighest tensile strength has been reported for graphene with young modulus value of 1TPa and strength of 130 GPA and stiffness similar to graphite [30].Raman spectroscopy has been used to investigate the intrinsic mechanical properties by monitoring the frequency of phonons under hydrostatic and uniaxial tensile stress[31].application of stress has also been used to create the band gap in graphene as it displaces the atoms and changes the local charge density .Graphene has excellent heat transfer capability thermal conductivity measured 4840-5300 W/mK by confocal micro Raman spectroscopy [32].This is the highest thermal conductivity reported at room temperature. This is an added advantage as heat generated in electronic devices during operation needs to be dissipated for their proper working .The excellent thermal conductivity has been a feature of all allotropes of carbon like graphite carbon nanotubes and has been attributed to phonon scattering and strong C-C bonds.

2.2 GRAPHENE SYNTHESIS

Mass production of graphene of highly crystalline quality and free from defects on an industrial scale still possess a formidable challenge among researchers. Until this dream is realized graphene wouldn't be able to replace material in devices used in everyday life thus wasting the trove of exceptional electronic and structural properties it holds. Graphene fabrication can be categorized into two methods namely called top down approach and bottom up approach. In top down method van der wall forces that holds the graphite layers are annihilated to provide us with monolayer and few layer graphene sheets. This is mainly achieved by the micromechanical cleavage of graphite and exfoliation of graphite intercalated compounds (GICs) .While micromechanical cleavage is very labour intensive procedure, exfoliation requires great care in maintaining the sheet quality (low defects) and preventing the reattachment of flakes. In bottom up methods graphene flakes are grown on substrate from various sources of carbon. Both methodologies have their share of advantages, disadvantages and constraints associated with them. Low production and large number of steps involved in top down practice has restricted its application only to laboratory research, while high temperature is the essential requirement for high quality graphene production in bottom up approach thought they are still inferior in quality as compared to one's produced in top down. Prime concerns in quality mostly pertain to its electron mobility that are affected by method of fabrication used due to a number of defects and type of substrate employed in it.

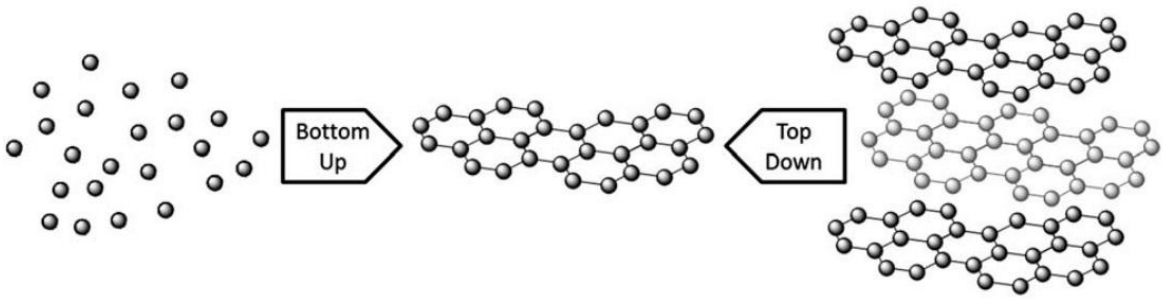

Fig2.6 Top down and bottom up graphene synthesis scheme [33]

The choice of method also depends on the final technological application as there are varied requirements ranging from transparent electrodes to thin films employed in sensors whereas batteries and super capacitors require large amount of graphene platelets and nanosheets. This shows that while some properties are paramount to certain application, they have no such

utility in other application for example thermal conductivity is required in polymer composite but not as such in electrodes. In contrast electron mobility and chemical inertness are very important in every application and it is insured that they remain intact in every fabrication method. Moreover sometime the very nature of method affect the choice too for example silicon carbide (SiC) is used as insulating substrate if it is used in electronics devices that need to be operable at room temperature while if it is grown on a metal that will require an additional step of transferring to insulation substrate. All these considerations fairly affect the choice of method of synthesis.

Top down Approaches

2.2.1 MICROMECHANICAL CLEAVAGE.

Using this technique also called 'scotch tape method' and 'peel off method', K. S. Novoselov and A. K. Geim were the first ones who were able to isolate monolayer and few layer graphene (FLG) from highly oriented pyrolytic graphite (HOPG) which was used as a precursor. Adhesive tape was used to tear apart the layer in successive manner by overcoming the weak van der wall forces that holds the layers together .Flakes were then transferred on SiO_2/Si (300 nm oxide layer) substrate and observed under optical microscope. As there was no characterization technique available for graphene at that time and graphene is almost transparent, it was no less than a serendipity that they were found. It was due to change in the refractive index and colour of the silicon oxide substrate and graphene layer when they were deposited on them. Monolayer, bi-layer, tri-layer and few layer graphene of very high quality can be obtained by this technique and easily characterized by this as they all change the colour of the substrate to different one. Synthesis by any other method does yield does not such high quality graphene but still its application is only limited principle research owing to tedious labour it requires and abrupt edges in final product.

2.2.2 EXFOLIATION TECHNIQUE

High hope are pinned on this technique for mass production of graphene though there are still some issues that needed to be tackled. This technique mainly deals with exfoliation of graphene intercalation compounds and graphene oxide .Exfoliation works by inserting foreign molecules between the layers and widening the gap thus weakening the inter layer attractive forces. This helps in breaking the predecessor

material into individual graphene layers.one such method is to use sulphuric acid – potassium hydroxide [34] with surfactant [35] and graphite. $[SO_4]^{2-}$ ions are responsible for intercalation thus making H_2SO_4 a good electrolyte whereas surfactant prevent stockpiling of sheets though they can tough to detach later[35] alongside adversely affecting graphene layer's electronic properties. Flakes of different thickness are then separated by centrifugation.

Graphite intercalation compounds which are formed by reaction of reducing agents or oxidising agent or salts with graphite followed by sonication in solvents or thermal expansions or gaseous expansions.

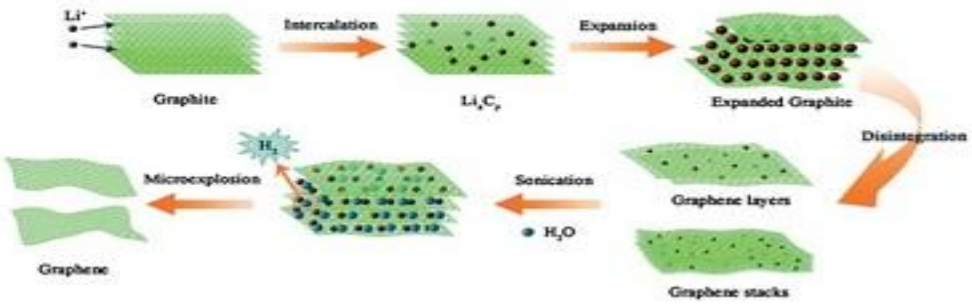

Figure 2.7 Sketch showing formation steps of graphene sheets through Li intercalation-expansion-micro explosion processes[36]

Bottom upApproaches

2.2.3 EPITAXIAL SILICON CARBIDE GROWTH

Graphene can be synthesised by the thermal decomposition of silicon carbide at very high temperature followed by subsequent rearrangement of carbon atoms to form graphene layers that are left behind after the sublimation of silicon atoms from top of the surface [17].Process requires very high temperatures (excess of 1000 ^oC) and ultra-high vacuum conditions though growth in inert gas atmosphere (argon) has been demonstrated too [37]. Different conditions produces different type of graphene with different properties varying in thickness and defects. Argon allows the use of higher temperature (1500 ^oC) that benefits in much better quality graphene as it drastically lower the rate of silicon sublimation making carbon atom more

mobile[b44].Hexagonal silicon carbide is generally used for graphene fabrication .Both carbon rich and silicon rich surface can be used synthesis and both results in graphene with varying quality levels. Si rich surface requires higher temperature thus giving better quality graphene of usually few layers that exhibits Bernal stacking [38] and that's why it is more studied of two. While carbon surface exhibits rotational stacking [38] requiring low temperatures and giving graphene with more layers (>10).Major challenges in this method includes the stringent requirements of high temperature and vacuum conditions.

Though nickel catalysed low temperature growth (700-800 ^{o}C) has been demonstrated but this spikes up the cost of fabrication owing to the costly transition metal nickel [39].This method is most suitable for the wafer based electronics devices as there is no need to transfer graphene on insulating substrate. Moreover it would be interesting to see how this method is used in economically viable devices as SiC is costly material.

2.2.4 CHEMICAL VAPOUR DEPOSITION

Carbon rich gases are broken down using pyrolysis at very high temperature in this method to grow monolayer and few layer graphene. Chemical vapour deposition can be divided into two routes where in first route the carbon containing gases are decomposed on the metal substrate to form monolayer graphene through surface catalyses and in other routes formation occurs by the segregation of carbon dissolved in metal bulk .the segregation on the top of metal surface upon cooling as solubility of carbon is decreased to a very low level giving multi-layer graphene which can be controlled by the cooling rate and the quantity of carbon dissolved in metal and their alloys namely with growth conditions and graphene quality varying from metal to metal .Nickel and Copper have been extensively used and researched for chemical vapour deposition of graphene .Graphene growth on nickel occurs through the segregation method in which the mixture of methane and hydrogen is decomposed on the nickel bulk and dissolved in it temperature above the 1000 ^{o}C . When the bulk is cooled down the metal precipitates out of the bulk and segregate on the surface of metal forming few layer graphene. Different rate of bringing down the temperature in this method greatly affects the quality and thickness of graphene in addition to obliterating the requirement of high vacuum conditions .On copper the growth occurs through the decomposition of carbon rich gas on its surface. This is due to the fact the

solubility of carbon is very low in copper metal and thus forming a monolayer of graphene on the copper substrate.

The major concerns that remains in this method are cost and availability of the transition metal that is going the affect the economics of the devices. The interaction between the metal and carbon also need to be taken care as metal has to be scratched off without damaging the graphene layer mostly done by spin coating technique. Other disadvantages in this method include high temperature and vacuum conditions required.

2.3 GRAPHENE CHARACTERIZATION TECHNIQUES

2.3.1 OPTICAL MICROSCOPY

This was the technique that was used to identify and characterize the graphene first time. Samples were put on silicon oxide having width 300nm were identified as there was change in light intensity that is reflected .The real magic lies in the width of substrate that is reflected .The real magic lies in the width of substrate that is 300nm that gives change in contrast due to interference of light at the junction that can be detected by human eye and even a slight change of 20 nm in width can render them invisible .This makes it the most effective techniques but labour intensive to readily characterize the mechanically exfoliated graphene in laboratory .The contrast can be as large as 12% due to additional optical path created by the graphene layer also depends on the wavelength of incident light and angle. The monolayer bilayer and few layer can be easily identified as they show different colour.

2.3.2 ATOMIC FORCED MICROSCOPY

This was the first technique to ascertain the fact that the flakes characterized by optical microscopy were truly the monolayer graphene .There is difference in the thickness of graphene that is found when it is placed on graphite crystal and when it is placed on silicon substrate .Where it is 0.4nm in former case and 0.8-1.2 thick in later .Thickness increases by 0.35 with each layer added that corresponds to Van der Waal distance between the layers.It’s still can’t be explained clearly why it shows extra thickness when placed ion silica. Though the AFM technique is slow and constrained in screen size, it is still best way to examine the topological properties graphene supported on substrate.

2.3.3 RAMAN SPECTROSCOPY

Raman spectroscopy has emerged as a characterization important tool that is used to probe graphene phonon spectrum. Density of defects, number of graphene layers, stacking order and impurities can be easily determined using the Raman spectroscopy. The most important bands in graphene Raman spectra and G bands at around 1580 cm^{-1} and D band at 2680 cm^{-1}. G band results from sp^2 atom in- plane vibration and is almost distinct for every graphitic material band's intensity directly corresponds to the defects in graphene lattice. Number of defect in graphene layer is estimated by calculating the ratio of G and D band intensities. Single layer graphene has highest intensity peak in G band with decreasing intensity with each addition of layer and no distinction in G band of 10 layer graphene and graphite.

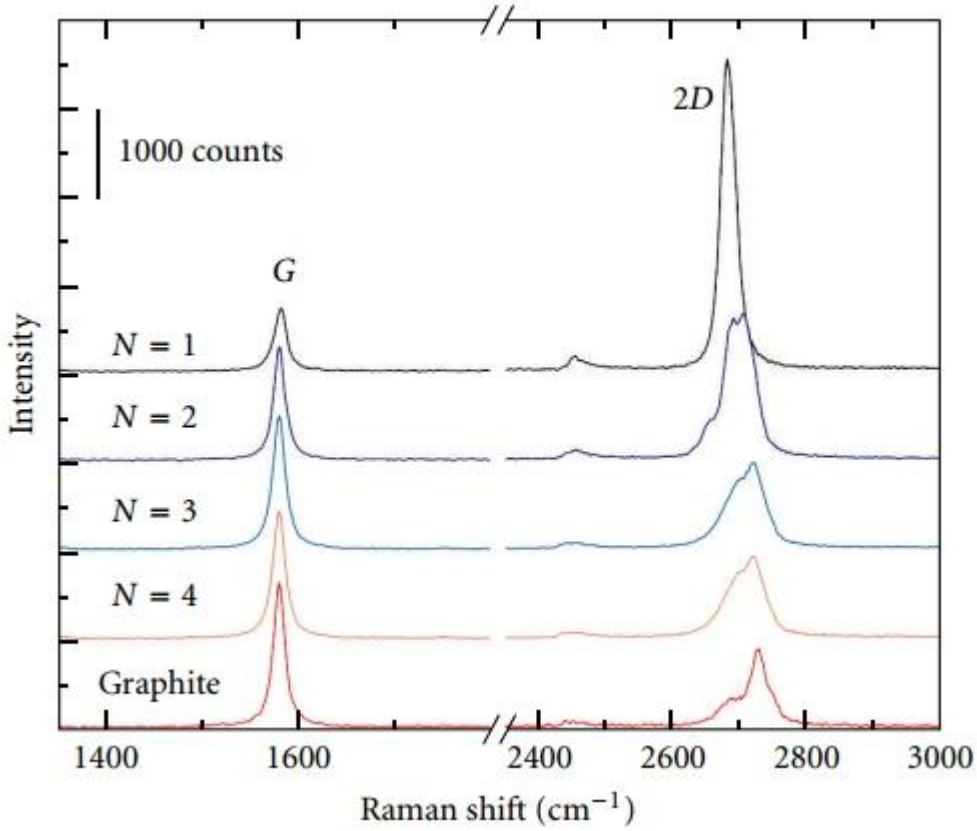

Figure 2.8 Raman Spectra of graphene with different width

2.4 GRAPHENE APPLICATIONS

2.4.1 MEDICINE

Graphene is being investigated as a reinforcing agent in tissue engineering applications considering its tensile strength and other highly rated mechanical properties .When graphene in powdered form is mixed in polymer matrix, crosslinking density is improved in nanocomposite thus imparting them better load handling capability. It has also being tried as a contrasting agent for magnetic resonance imaging and thermo acoustic tomography .it has also been reported that due to its thermal conductivity it can also catalysed polymerase chain reaction through the increase of DNA product yield. Graphene has a large surface area and can be easily be modified and bent thus finding application in bio sensors and diagnosis devices. It has been also found the low level concentration of graphene nanoribbons are nontoxic in nature and does not harm the stem cells ,therefore can be used for drug delivery system in cancer treatment to kill cancerous cells.

2.4.2 ELECTRONICS

Most of the future of graphene is seen in the field of electronic devices given its high carrier mobility and associated low noise. Graphene has ability to replace silicon in electronics devices with much faster speed and smaller size if its limitations are removed. Gated graphene has low on/off ratio of order around 10 depending on graphene's quality and gating effectiveness, while to make digital switch the ratio required in digital transistor is 10^4.This can be attributed to its zero band gap property. This is biggest hurdle in its way to become an effective logic gate. A lot of research has been done in this field to open a band gap including quantum confinement in graphene by cutting into nanoribbons but no major breakthrough has been achieved in this field. IBM has already designed and fabricated graphene based transistor and integrated circuit which is a broadband mixer that can work up to of frequencies of 10 GHz and temperature of 127 ^oC though it suffer from low voltage gain.Graphene also have a great potential to substitute for indium tin oxide as a transparent conducting film in solar devices, light emitting diodes and other displays. Given ITO has available in limited quantity and due to its rising cost the need for replacement is greater than ever. Merits of graphene in this case include higher optical transparency (98%) than ITO (90%) and mechanical flexibility whereas ITO is brittle. That's why graphene can find great

application in wearable electronics. Only hurdle in this application is its very high electrical resistance offered by graphene sheets than ITO. Some progress in this direction to reduce resistance has been made by increasing the number of layers and treating with nitric acid both at the cost of reduced transparency. Hall effects sensors with very high sensitivity have been developed from graphene that may find applications with DC current transformers. Graphene fabricated using chemical vapour deposition technique on SiO_2 substrate has been found to preserve their spin for a long time and this can be used in spintronics application where spin is used a data at the place on current state. This can be used in data storage disks and magnetic random access memory. It shows sensitivity to infrared spectrum at room temperature and thus can also be effectively used in infrared devices and contact lenses.

2.4.3 ENERGY

Membranes of graphene oxide is impermeable to gases and liquid but allow water vapour to pass through it. This property has been used to effectively distil alcohol to higher concentration at room temperature with traditional vacuum distillation method and can be further utilized into better biofuel economies. Graphene's high optical transparency and electron mobility find great application in solar devices with better conversion efficiency than silicon based devices. It is also found that graphene let protons pass through it thus raising the hopes for better and efficient fuel cells .Considering graphene large surface area one potential application is in super capacitors' conductive plates .Graphene based micro super capacitors have been demonstrated .

CHAPTER 3

COMPUTATIONAL METHODOLOGY

3.1 DENSITY FUNCTIONAL THEORY

Density functional theory is a computational method that uses quantum mechanics model to solve the many body system primarily to investigate there ground structure and usually find there electronics properties. It has been successfully applied in the condensed physics and molecular chemistry world.The ultimate goal of most approaches in solid state physics and quantum chemistry is the Solution of the time-independent, non-relativistic Schrodinger equation.The quantum mechanical wave function contains, in principle, all the information about a given system. For the case of a simple 2-D square potential or even a hydrogen atom we can solve the Schrödinger equation exactly in order to get the wave function of the system. We can then determine the allowed energy states of the system. Unfortunately it is impossible to solve the Schrödinger equation for a N-body system. Evidently, we must involve some approximations to render the problem soluble albeit tricky. Here we have our simplest definition of DFT: A method of obtaining an approximate solution to the Schrodinger equation of a many-body system.

$$\hat{H}\,\Psi_i(\vec{x}_1,\vec{x}_2,\ldots,\vec{x}_N,\vec{R}_1,\vec{R}_2,\ldots,\vec{R}_M) = E_i\,\Psi_i(\vec{x}_1,\vec{x}_2,\ldots,\vec{x}_N,\vec{R}_1,\vec{R}_2,\ldots,\vec{R}_M)$$

$\hat{H}$ is the Hamiltonian for a system consisting of M nuclei and N electrons.

$$\hat{H} = -\frac{1}{2}\sum_{i=1}^{N}\nabla_i^2 - \frac{1}{2}\sum_{A=1}^{M}\frac{1}{M_A}\nabla_A^2 - \sum_{i=1}^{N}\sum_{A=1}^{M}\frac{Z_A}{r_{iA}} + \sum_{i=1}^{N}\sum_{j>1}^{N}\frac{1}{r_{ij}} + \sum_{A=1}^{M}\sum_{B>A}^{M}\frac{Z_A Z_B}{R_{AB}}$$

Here, A and B run over the M nuclei while i and j denote the N electrons in the system. The first two terms describe the kinetic energy of the electrons and nuclei. The other three terms represent the attractive electrostatic interaction between the nuclei and the electrons and repulsive potential due to the electron-electron and nucleus-nucleus interactions.

Born-Oppenheimer approximation: due to their masses the nuclei move much slower than the electrons so we can consider the electrons as moving in the field of fixed nuclei and the nuclear kinetic energy is zero and their potential energy is merely a constant. Thus, the electronic Hamiltonian reduces to

$$\hat{H} = -\frac{1}{2}\sum_{i=1}^{N}\nabla_i^2 - \sum_{i=1}^{N}\sum_{A=1}^{M}\frac{Z_A}{r_{iA}} + \sum_{i=1}^{N}\sum_{j>1}^{N}\frac{1}{r_{ij}} = \hat{T} + \hat{V}_{Ne} + \hat{V}_{ee}$$

The solution of the Schrodinger equation with $\hat{H}_{elec}$ is the electronic wave function Ψ_{elec} and the electronic energy $\hat{E}_{elec}$. The total energy $\hat{E}_{tot}$is then the sum of $\hat{E}_{elec}$and the constant nuclear repulsion term $\hat{E}_{nuc}$.

$$\hat{H}_{elec}\,\Psi_{elec} = \hat{E}_{elec}\,\Psi_{elec}$$

$$E_{tot} = E_{elec} + E_{nuc} \text{ Where } E_{nuc} = \sum_{A=1}^{M}\sum_{B>A}^{M}\frac{Z_A Z_B}{R_{AB}}$$

3.1.1 The variational principle for the ground state

When a system is in the state Ψ, the expectation value of the energy is given by

$$E[\Psi] = \frac{\langle\Psi|\hat{H}|\Psi\rangle}{\langle\Psi|\Psi\rangle} \text{where} \langle\Psi|\hat{H}|\Psi\rangle = \int \Psi^{*}\,\hat{H}\Psi\, d\vec{x}$$

The variational principle states that the energy computed from a guessed Ψ is an upper bound to the true ground-state energy E_0. Full minimization of the functional $E[\Psi]$ with respect to all allowed N-electrons wave functions will give the true ground state Ψ_0 and energy$E[\Psi_0]$ = E_0; that is

$$E_0 = min_{\Psi\to N}E[\Psi] = min_{\Psi\to N}\langle\Psi|\hat{T} + \hat{V}_{Ne} + \hat{V}_{ee}|\Psi\rangle$$

For a system of N electrons and given nuclear potential V_{ext}, the variational principle defines a procedure to determine the ground-state wave function Ψ_0, the ground-state energy $\mathbf{E_0\,[N, V_{ext}]}$, and other properties of interest. In other words, the ground state energy is a functional of the number of electrons N and the nuclear potential $\mathbf{V_{ext}}$:

$$E_{0=}E[N, V_{ext}]$$

3.1.2 The Electron density

The electron density is the central quantity in DFT. It is defined as the integral over the spin coordinates of all electrons and over all but one of the spatial variables $(\vec{x} \equiv \vec{r}, \mathbf{s})$.

$$\rho(\vec{r}) = N\int \ldots \int |\Psi(\vec{x}_1, \vec{x}_2, \ldots., \vec{x}_N|^2 ds_1 d\vec{x}_2 \ldots.. d\vec{x}_N$$

$\rho(\vec{r})$ determines the probability of finding any of the N electrons within volume element $d\vec{r}$.

The first Hohenberg-Kohn theorem: The first Hohenberg-Kohn theorem demonstrates that the electron density uniquely determines the Hamiltonian operator and thus all the properties of the system.

This first theorem states that the external potential $\mathbf{V_{ext}}(\vec{r})$ is (to within a constant) a unique functional of $\rho(\vec{r})$; since, in turn $V_{ext}(\vec{r})$ fixes Hˆ we see that the full many particle ground state is a unique functional of $\rho(\vec{r})$.$\rho(\vec{r})$ determines N and $V_{ext}(\vec{r})$ and hence all the properties of the ground state, for example the kinetic energy T[ρ], the potential energy V [ρ], and the total energy E[ρ]. Now, we can write the total energy as

$$\boldsymbol{E[\rho] = E_{Ne}[\rho] + T[\rho] + E_{ee}[\rho] = \int \rho(\vec{r}) V_{Ne}(\vec{r}) d\vec{r} + F_{HK}[\rho]}$$

$$\boldsymbol{F_{HK}[\rho] = T[\rho] + E_{ee}}$$

This functional FHK[ρ] is the holy grail of density functional theory. If it were known we would have solved the Schrodinger equation exactly! And, since it is a universal functional completely independent of the system at hand, it applies equally well to the hydrogen atom as to gigantic molecules such as, say, DNA! FHK[ρ] contains the functional for the kinetic energy T[ρ] and that for the electron-electron interaction, E_{ee}[ρ]. The explicit form of both these functional lies completely in the dark. However, from the latter we can extract at least the classical part J[ρ],

$$\mathbf{E_{ee}[\rho] = \frac{1}{2} \int \int \frac{\rho(\vec{r}) \rho(\vec{r})}{r_{12}} d\vec{r}_1 d\vec{r}_2 + E_{ncl} = J[\rho] + E_{ncl}[\rho]}$$

Encl is the non-classical contribution to the electron-electron interaction: self-interaction correction, exchange and Coulomb correlation. The explicit form of the functional **T[ρ]** and $\mathbf{E_{ncl}[\rho]}$ is the major challenge of DFT.

The second Hohenberg-Kohn theorem: The second H-K theorem states that **FHK[ρ],** the functional that delivers the ground stateenergy of the system, delivers the lowest energy if and only if the input density is the true ground state density.

We have seen that the ground state energy of a system can be written a

$$\boldsymbol{E_0 = min_{\rho \to N} (F[\rho] + \int \rho(\vec{r}) V_{Ne} d\vec{r}}$$

Where the universal functional F[ρ] contains the contributions of the kinetic energy, the classical Coulomb interaction and the non-classical portion:

$$\boldsymbol{F[\rho] = T[\rho] + J[\rho] + E_{ncl}[\rho]}$$

Of these, only **J[ρ]** is known. The main problem is to find the expressions for **T[ρ]** and $\mathbf{E}_{ncl}\mathbf{[\rho]}$.Kohn and Sham accounted for that by introducing the following separation of the functional **F[ρ]**

$$\boldsymbol{F[\rho] = T_s[\rho] + J[\rho] + E_{XC}[\rho]}$$

Where E_{XC}, the so-called exchange-correlation energy is defined through Equation below

$$\boldsymbol{E_{XC}[\rho] = (T[\rho] - T_s[\rho] + J[\rho])}$$

The exchange and correlation energy E_{XC} is the functional that contains everything that is unknown.To solve this problem, we write down the expression for the energy of the interacting system in terms of the separation

$$\boldsymbol{E[\rho] = T_s[\rho] + J[\rho] + E_{XC}[\rho] + E_{Ne}[\rho]}$$

The two difficult terms to calculate here are the kinetic energy and the exchange correlation energy.An approximation to the exchange-correlation term is used. It is called the Local Density Approximation (LDA). For any small region, the exchange-correlation energy is the approximated by that for jellium of the same electron density. In other words, the exchange-correlation hole that is modelled is not the exact one - it is replaced by the hole taken from an electron gas whose density is the same as the local density around the electron.

The interesting point about this approximation is that although the exchange-correlation hole may not be represented well in terms of its shape, the overall effective charge is modelled exactly. This means that the attractive potential which the electron feels at its centre is well described. Not only does the LDA approximation work for materials with slowly varying or homogeneous electron densities but in practise demonstrates surprisingly accurate results for a wide range of ionic, covalent and metallic materials. An alternative, slightly more sophisticated approximation is the Generalised Gradient Approximation (GGA) which estimate the contribution of each volume element to the exchange-correlation based upon the magnitude and gradient of the electron density within that element. The kinetic energy term could easily be calculated by using the same principle as LDA. That is, we could use the result derived from a homogeneous electron gas. This is the approach followed by Thomas Fermi theory. Unfortunately, the accuracy needed to describe the small energy changes that characterise chemical bonding is not sufficient with this approach. We need another way of getting the kinetic energy.

Two clever chaps, Kohn and Sham introduced a set of orbitals from which the electron density can be calculated. These Kohn-Sham orbitals do not, in general, correspond to the actual electron orbitals. Likewise, the Kohn-Sham eigenvalues are not in general the same as the real energy levels. The only connection the Kohn-Sham orbitals necessarily have to the real electronic wave functions is that they both give rise to the same charge density. The Kohn-Sham orbitals are used to calculate the kinetic energy. The property of the orbitals that makes them useful in the derivation is their orthonormality. The tricky problem of a system of interacting electrons has now been mapped onto that of a system of non-interacting electrons moving in an effective potential.

3.2 COMPUTATIONAL DETAILS

The analysis of the structural stability and electronics properties of the Mn and Cr terminated AGNR has been carried out using the ab-initio approach within the frame work of the density function theory [40].All the calculation has been performed using Atomistix Toolkit-Virtual NanoLab (ATK-VNL), for simulation and analysis of physical and chemical properties of nano scale devices which is developed and sold commercially by Quantum Wise [41] It would be worthwhile to note that the ATK is the further development of the TranSIESTA-C, which in turn in based on the technology, models, and algorithms developed in the academic codes TranSIESTA[42] and McDCal [43] employing localized basis sets as developed in SIESTA. To account for the exchange and correlation term, we have used the local density approximation as proposed by the Perdew and Zenger[44].To represent the number of the plain wave basis sets , an energy cut off of 50 Rydberg was selected. Along with this, supercell geometry was used in which the Nanoribbons were modeled along the z-direction and with suitable vacuum created along the other x and y directions to avoid interaction between nanoribbons and its periodic image. Maintaining self-consistency throughout the calculations we have used 1 × 1× 50 Monkhorst- pack grid in one dimensional Brillouin zone. In agreement with aforementioned condition, the atoms were relaxed and free to displace their position till force less than 0.05 eV/Å was achieved.Figure 3.1 shows sites of termination of single and double edge in ribbons with encircled atoms being replaced with Mn and Cr.

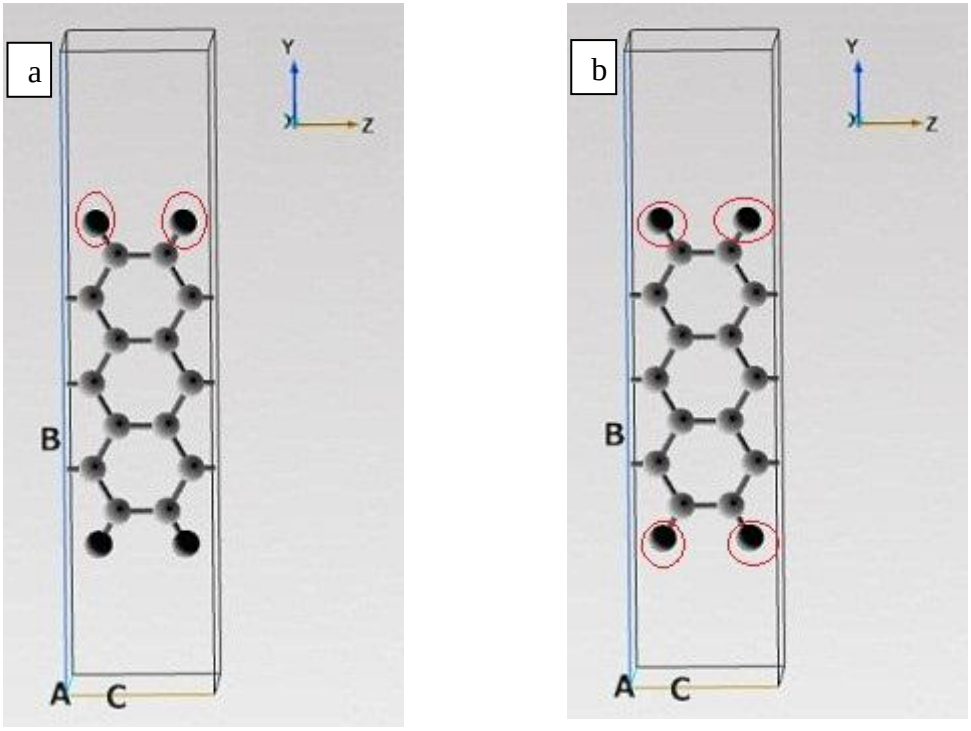

Figure 3.1 Sites of termination (a) single edge termination (b) double edge termination

CHAPTER 4

RESULTS AND DISCUSSION

4.1 STRUCTURAL STABILITY

We have analysed the stability of the width Na =4-9 AGNRs terminated with Mn and Cr impurities by finding binding energy per atom and also investigated their electronics properties. Two Different sites (single edge and double edges) have been adopted for the Mn and Cr termination in all Configurations.

Firstly the ground state analysis of different width AGNRs has been performed on the basis of total energy calculation. Next, to study stability of Mn/Cr-AGNR binding, we calculated the binding energies defined as the energy required to assemble the atoms in the system of all the configurations aforementioned. Binding Energy is calculated as per the formula E_b =E(Mn/Cr-AGNR)-E(AGNR)-nE(Mn/CR)+nE(H),whereE(Mn/Cr-AGNR), E(AGNR) are respectively the total energies of the of Mn or Cr terminated AGNRs and H-terminated AGNR. E(Mn/Cr) is the total energy of the isolated energy of Mn or Cr atom whichever is used in the configuration and 'n' is the number of the terminating atoms per unit cell of the ribbon. Lower the binding energy of the configuration, more stable it is. Binding energies of the configurations have been shown in table 1.

Table 1
Binding energy per atom as a function of ribbon width with different terminations

Width(N_a)	**Binding energy (eV)**			
	Mn-termination single edge	Cr-termination single edge	Mn-termination double edge	Cr-termination double edge
4	-7.236	-16.344	-7.194	-16.434
5	-7.264	-16.382	-7.167	-16.372
6	-7.224	-16.341	-7.170	-16.487
7	-7.164	-16.355	-7.158	-16.330
8	-7.235	-16.338	-7.205	-16.348
9	-7.169	-16.345	-7.164	-16.344

Comparative analysis of binding energy calculations in table 1 throws up some interesting results though any general dependency on binding energy of any particular family can't asserted as only two width has been taken form each family of AGNRs .Minimum binding energy has been observed for the family of 3m+2 in case of Single edge terminated Mn-

AGNR ,where Na=5 is having BE= -7.264 eV as compared to 3m and 3m+1 families whose Na=3 is having BE = -7.224 eV and Na=5 is having BE =-7.236 eV indicating more stable nature.. Similarly binding energy of ribbon with Na = 8 (3m+2) family is 7.235 eV as compared to ribbons of width Na = 7 and 9 having binding energies -7.164 eV and -7.169 eV respectively. This shows that the Mn atoms are more tightly bound in 3m+2 family AGNRs and hence they are most stable configurations of all the single edge terminated Mn-AGNRs when compared to ribbons of the consecutive widths (4, 6) of other families. Contrary to above observation N_a=4 is slightly more stable than ribbon of width N_a=8 for double edge termination. It is also seen that 3m+1(N_a=4) family is more stable than 3m (N_a=6) family ribbon from configuration widths 4 to 6 and results is opposite from width 7 to 9 though the relative difference keep getting smaller .However the same conclusion can't be drawn in case of double edge terminated AGNR where binding energy is increasing and decreasing alternatively with increasing width. Results shows that 3m+1 is most stable with B.E. = -7.194 eV as compared to 3m and 3m+2 family which have BE energies -7.170 eV and -7.167 eV respectively in first three configuration (width 4 to 7) .In next three configuration N_a= 8 is most stable configuration followed by Na=9 and N_a=4 and overall N_a=4 is most stable configuration of all. Single edge terminations is more stable than double edge terminations in all ribbons .Moreover interestingly it can be seen that in all configurations binding energy increases as width (N_a) increases in respective families , evident from the observation that ribbon with width '4' is more stable that ribbon of width '7'.Similiar study has been performed on Cr- terminated AGNRs and found that in single edge termination N_a=5 is most stable followed by N_a=7 whereas N_a=6 is most stable configuration in double edge termination. We also found that Cr-terminated AGNRs are found to be more stable as compared to Mn-terminated ones.The bond length between the Mn and C atom is found to be 2.11 Å whereas the bond length between the edge carbon atoms has changed from 1.42 Å to 1.39. Bond length between Cr and C is found to be 2.272 Å.

4.2 ELECTRONIC BAND STRUCTURE ANALYSIS

Band structures have been analysed for the H-terminated, Mn-terminated and Cr-terminated AGNRs and results have been compared with the band structures of H-terminated AGNRs. Minimum band gap in case of H-terminated AGNRs have been found for the 3m+2 family of Nanoribbons , which is 0.252 eV for N_a =8 as compared to band gaps of all other configurations and all values calculated are in excellent agreement with previous theoretical

predictions [7] . All the band gap for the each configuration is shown in table 3 and table 4 below.

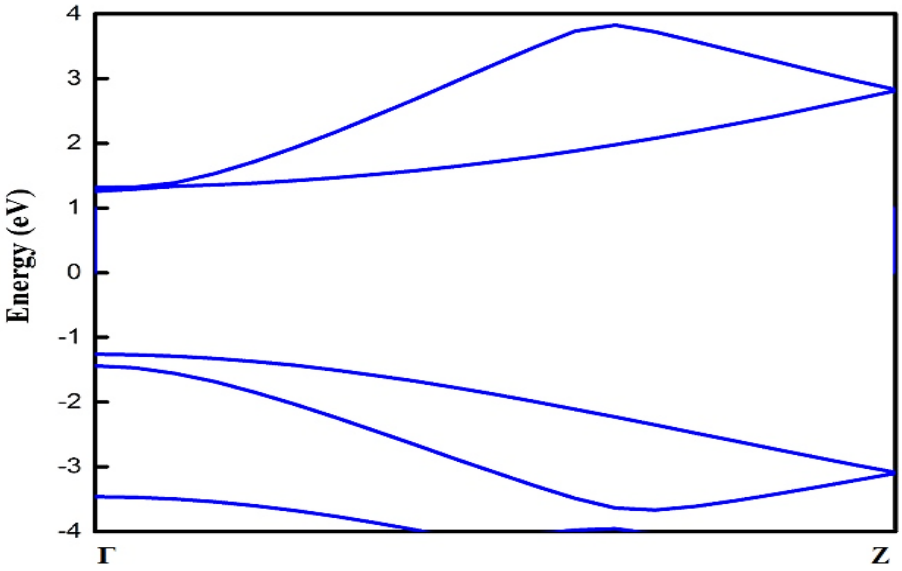

Figure 4.1 Band structure of pristine AGNR (N_a =4)

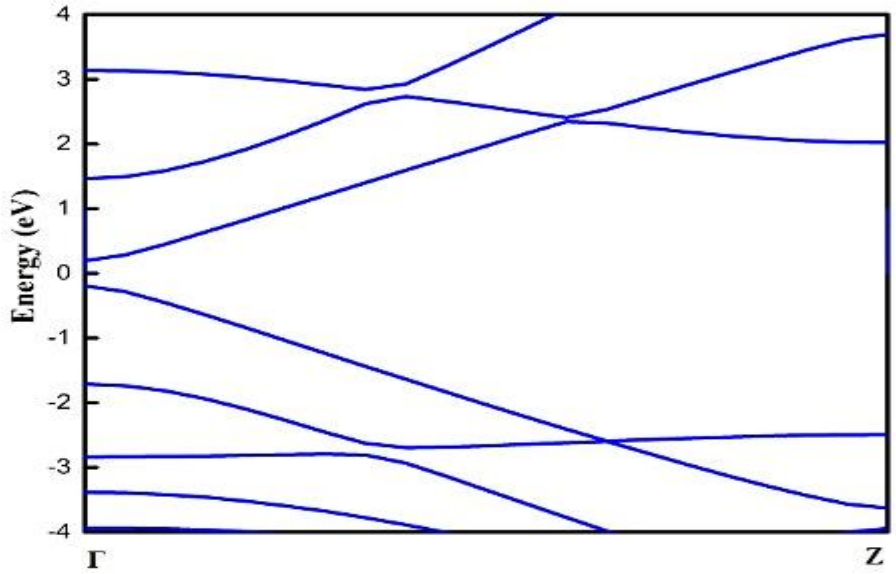

Figure 4.2 Band structure of pristine AGNR (N_a =5)

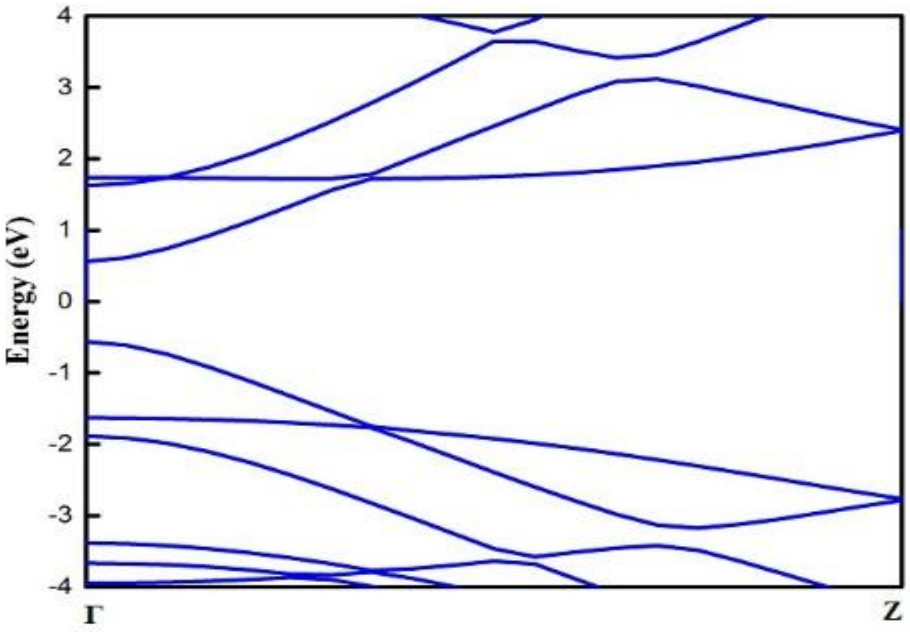

Figure 4.3 Band structure of pristine AGNR (N_a =6)

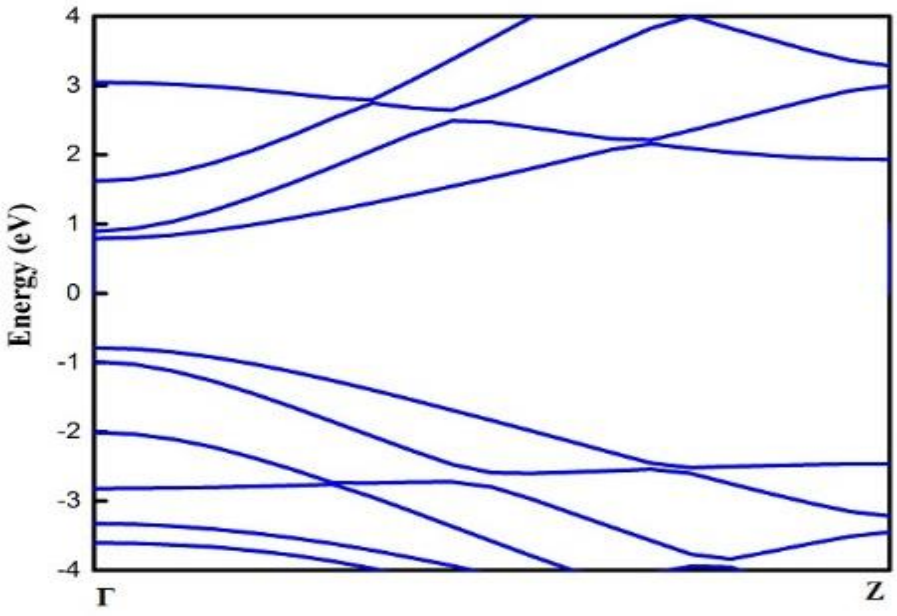

Figure4.4 Band structure of pristine AGNR (width =7)

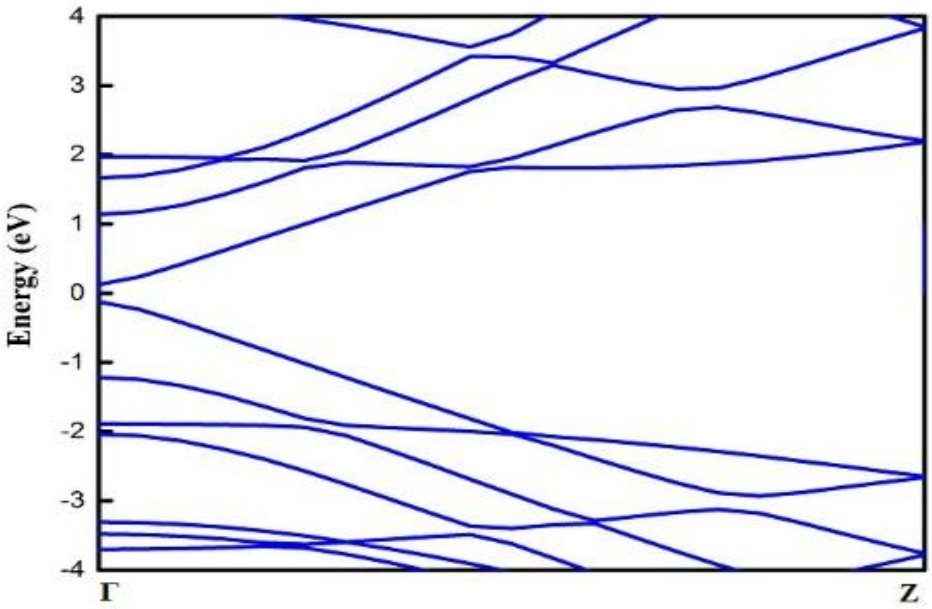

Figure 4.5 Band structure of pristine AGNR (width =8)

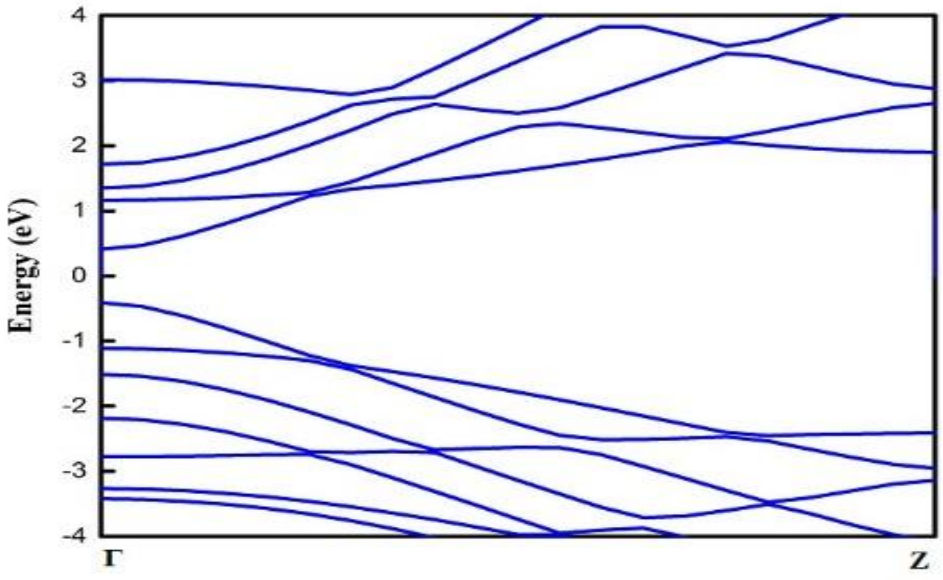

Figure 4.6 Band structure of pristine AGNR (N_a=9)

Table 2

Variation of the band gap as a function of ribbon widths for Mn and Cr termination

Width(N_a)	**Energy band gap(eV)**					
	H-termination		Mn-termination Single edge	Mn-termination double edge	Cr-termination double edge	Cr-termination double edge
	Present work	Other's calculation[7]				
4	2.52	2.53	0.635	0.600	0.233	0.5
5	0.39	0.43	0.439	0.387	0.138	Metallic
6	1.13	1.10	0.566	0.222	0.208	Metallic
7	1.57	1.58	0.642	0.584	0.237	0.167
8	0.25	0.27	0.327	0.304	Metallic	Metallic
9	0.82	0.80	0.350	0.209	0.133	Metallic

In single edge termination of Mn-AGNR of width N_a=4 and N_a =7that belongs to 3m+1 family we have found that band gap has significantly decreased from 2.52 eV to 0.635 eV. In two edge termination it has further reduced to 0.60 eV. Other ribbons of width N_a =7 of family too follows in the footstep of previous members with its band gap been reduced to 0.642 eV in single edge termination and 0.584 eV Single double edge termination from 1.574 eV in H-terminated configuration. Exactly Same pattern can be seen in 3m family of ribbon Na=6, where band gap has reduced from 1.126 eV to 0.566 eV in single edge termination and to 0.222 eV in double edge termination where 1.426 eV being the band gap of the H terminated configuration. Second member configuration (width N_a =9) exhibit same behaviour with its H terminated configuration's band gap 0.820 eV reduced to 0.350 eV and 0.209 respectively in single edge and double termination. However in ribbon with N_a=5, we have a diversion from above behaviour as in this case band gap increases in one edge termination but again slightly decreases in two edge termination, which is evident from the fact that in Mn-terminated ribbon of width N_a =5 the band gap has values 0.439 eV in single edge termination and 0.387 eV in double edge termination. While in width N_a =8 single edge termination has value 0.352 eV and double edge termination has value 0.304 eV as compared to band gap of 0.252 eV of H-terminated AGNRs. All the results shows that Mn-terminated ribbons have additional electronics states in conduction band and as well as valance band. In one edge termination minimum band gap is for 3m+2 family of ribbons as they already have lower band gap in pristine configurations but in case of both edge termination, an unusual behaviour is predicted as minimum band gap is for 3m family of AGNRs. Except for 3m+1

family ribbons all the band gap have been converted to indirect configuration from direct one in H-terminated ribbons. Band gaps of the various configurations of Mn-terminated armchair graphene nano ribbons are shown in figure 2.

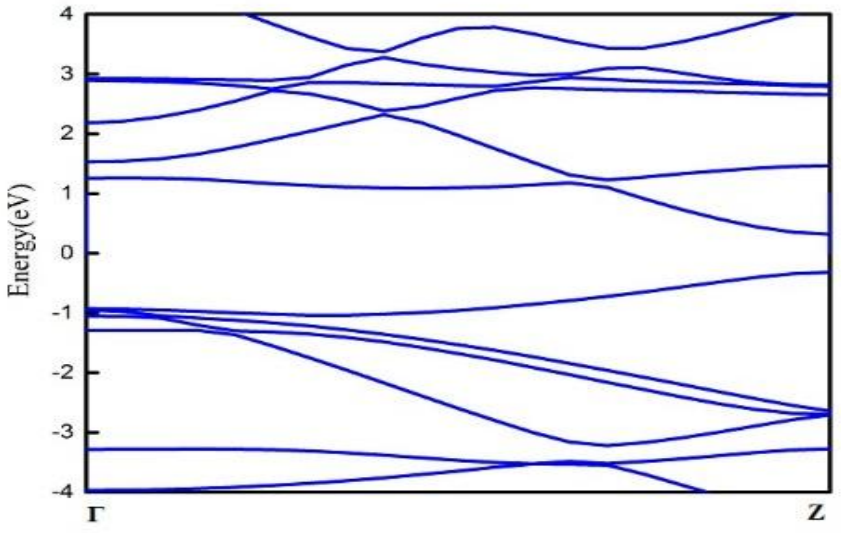

Figure 4.7 Band structure of single edge Mn terminated AGNR (N_a =4)

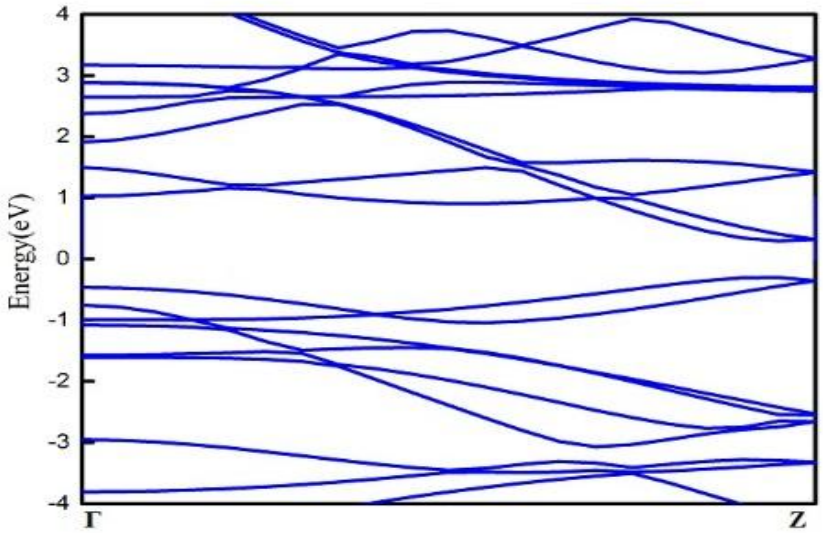

Figure 4.8 Band structure of double edge Mn terminated AGNR (N_a =4)

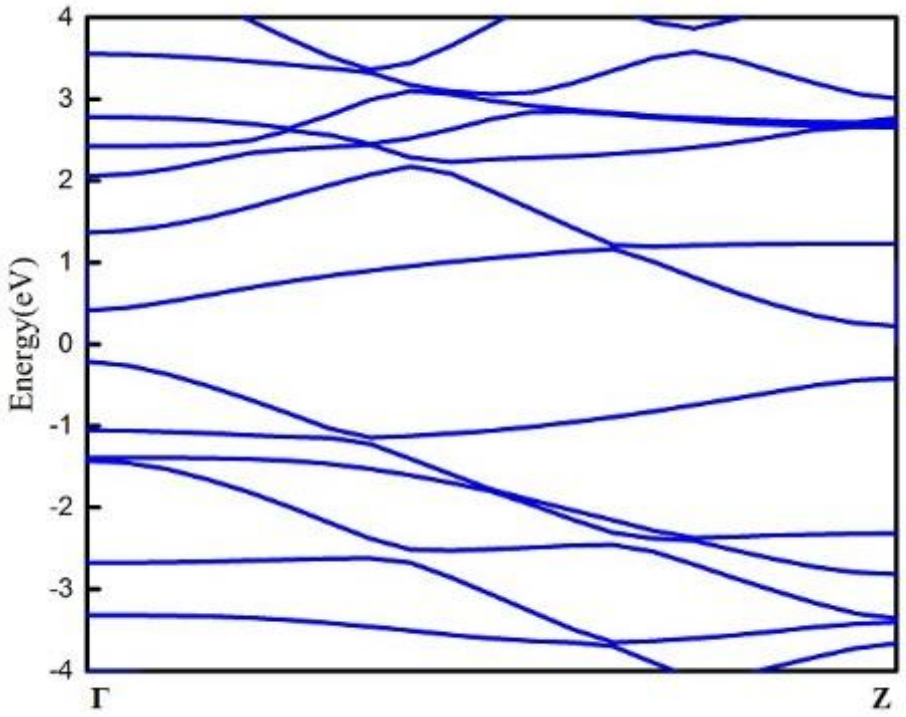

Figure 4.9 Band structure of single edge Mn terminated AGNR (N_a =5)

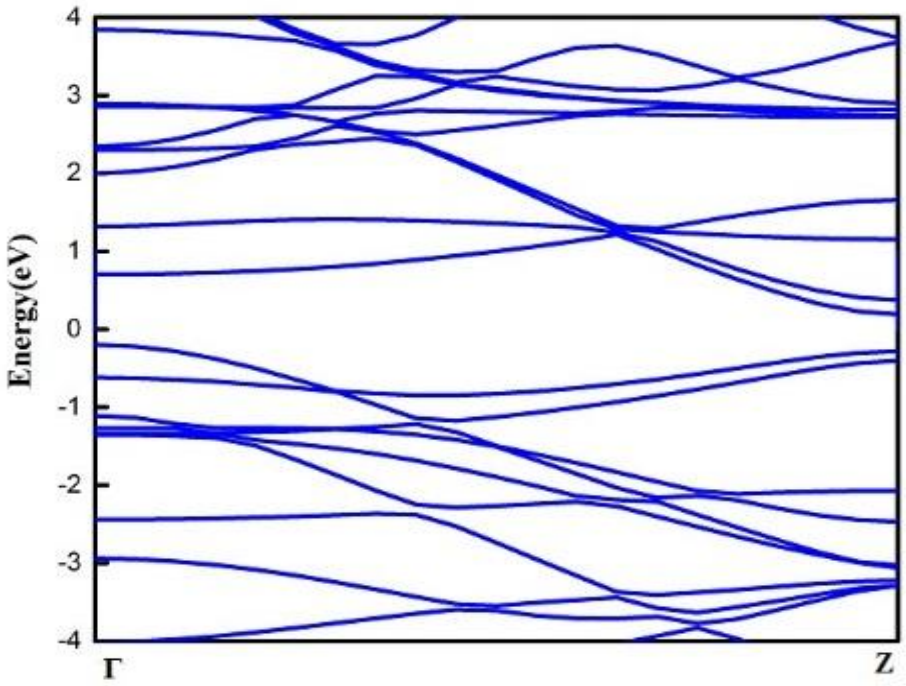

Figure 4.10 Band structure of double edge Mn terminated AGNR (N_a =5)

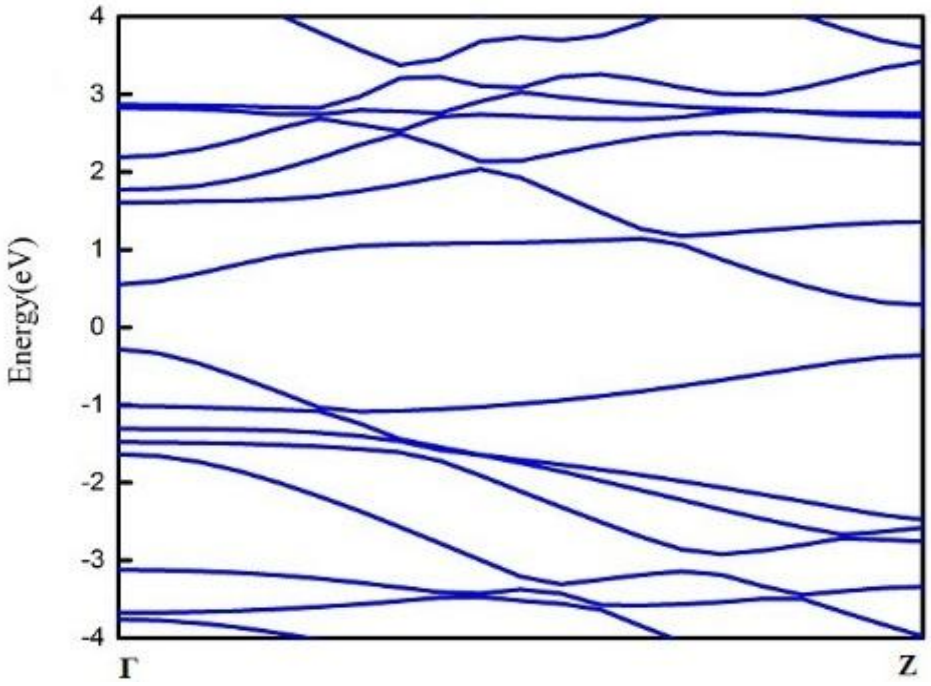

Figure 4.11 Band structure of single edge Mn terminated AGNR (N_a =6)

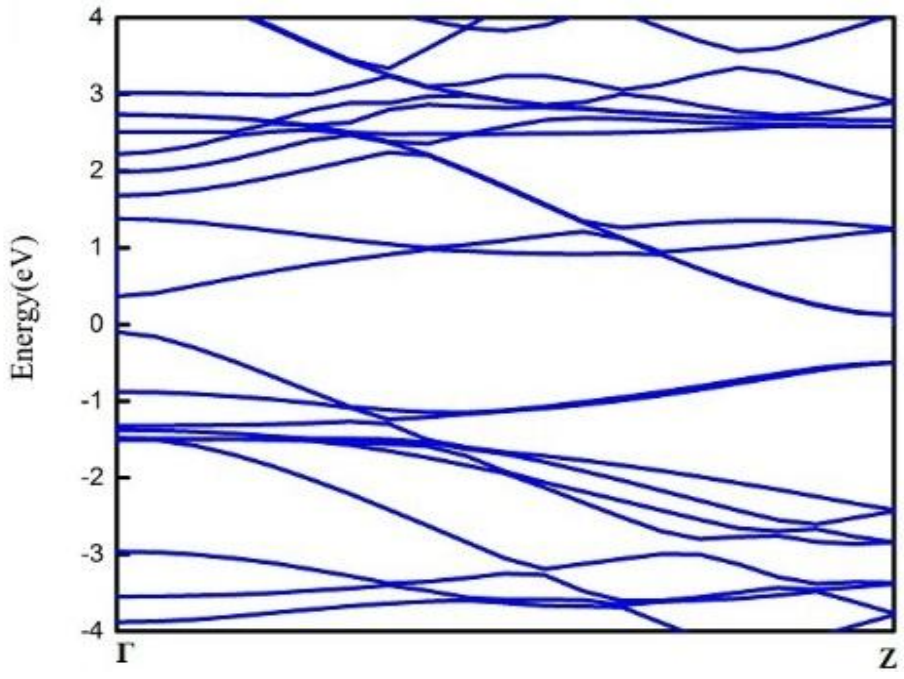

Figure 4.12 Band structure of double edge Mn terminated AGNR (N_a =6)

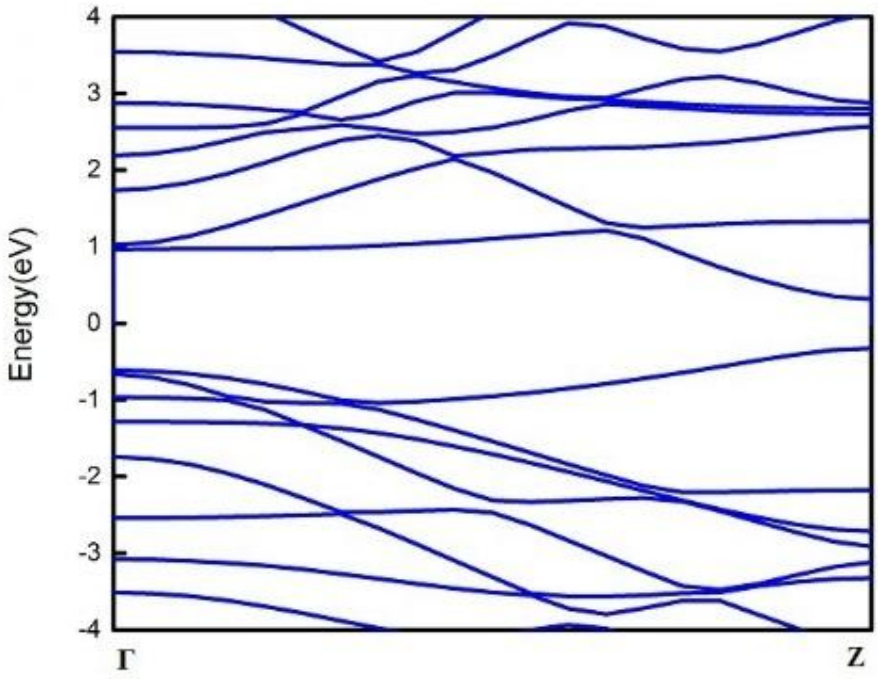

Figure 4.13 Band structure of single edge Mn terminated AGNR (N_a =7)

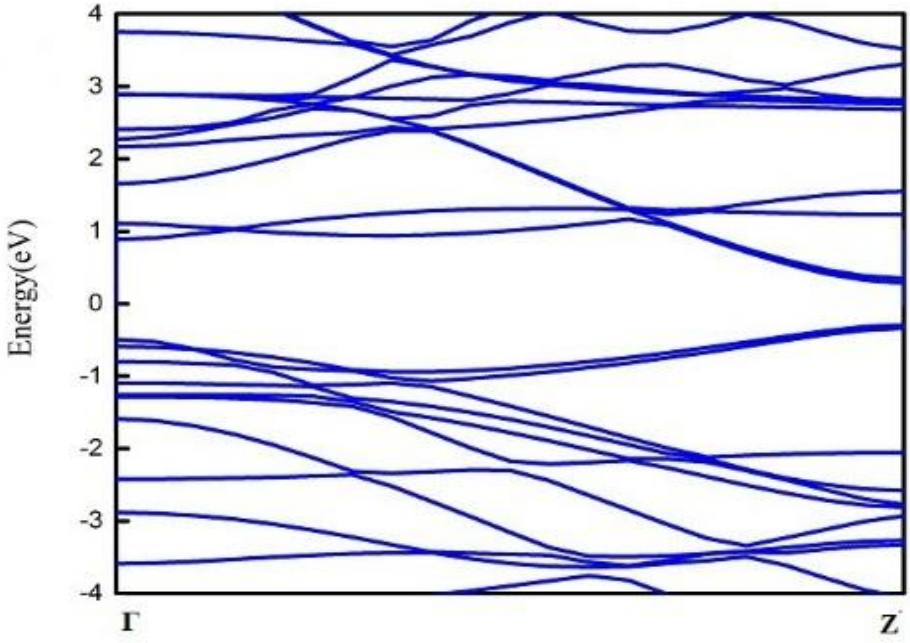

Figure 4.14 Band structure of double edge Mn terminated AGNR (N_a =7)

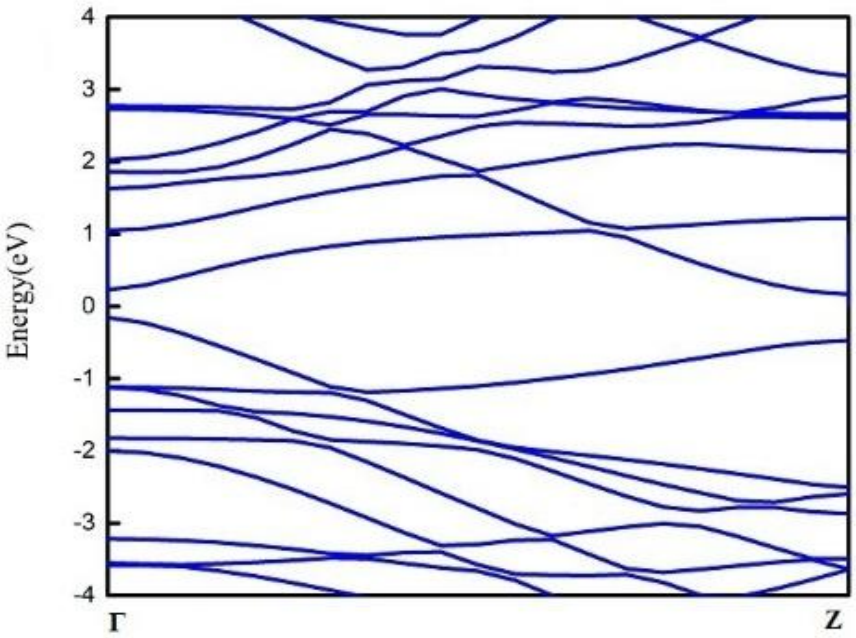

Figure 4.15 Band structure of single edge Mn terminated AGNR (N_a =8)

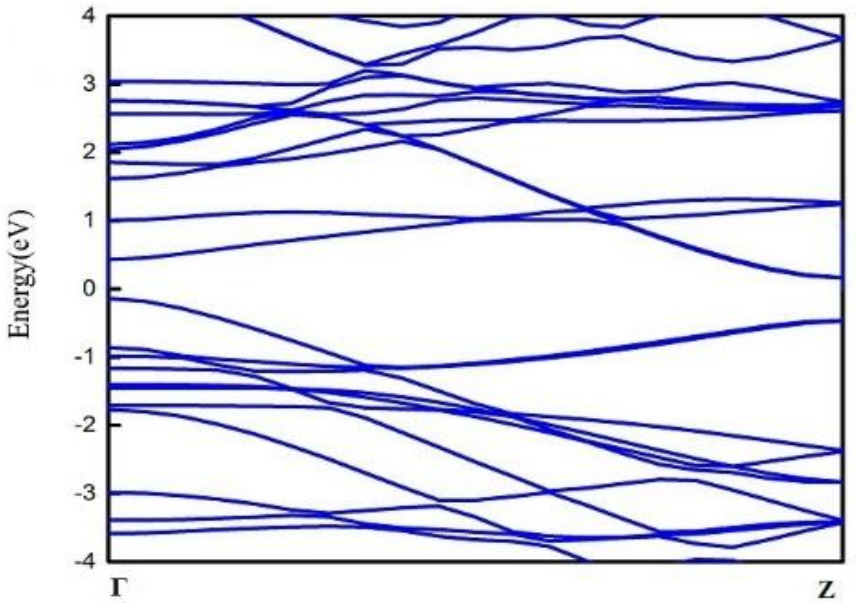

Figure 4.16 Band structure of double edge Mn terminated AGNR (N_a=8)

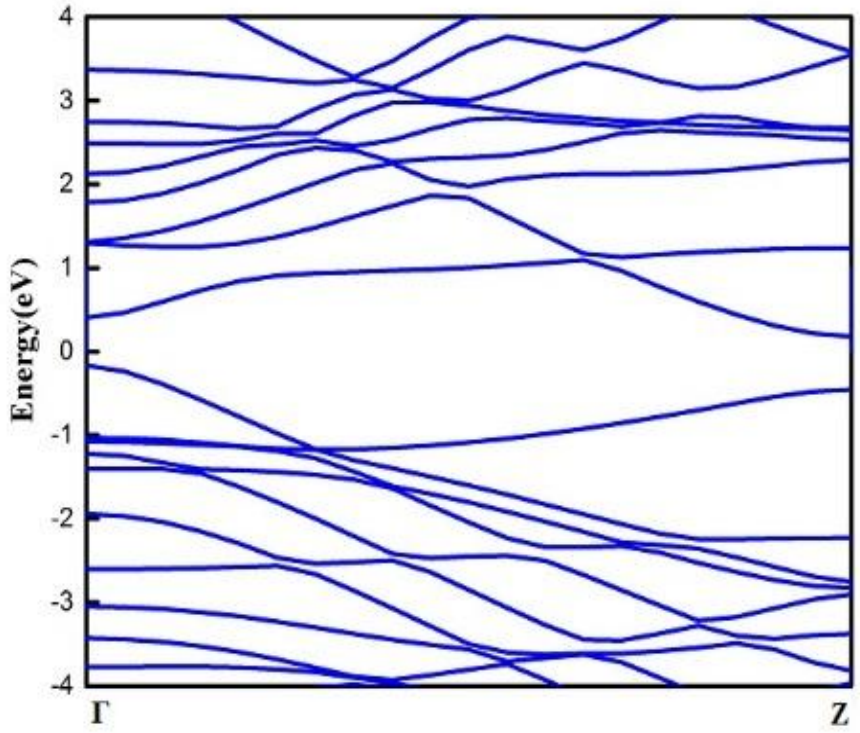

Figure 4.17 Band structure of single edge Mn terminated AGNR (N_a =9)

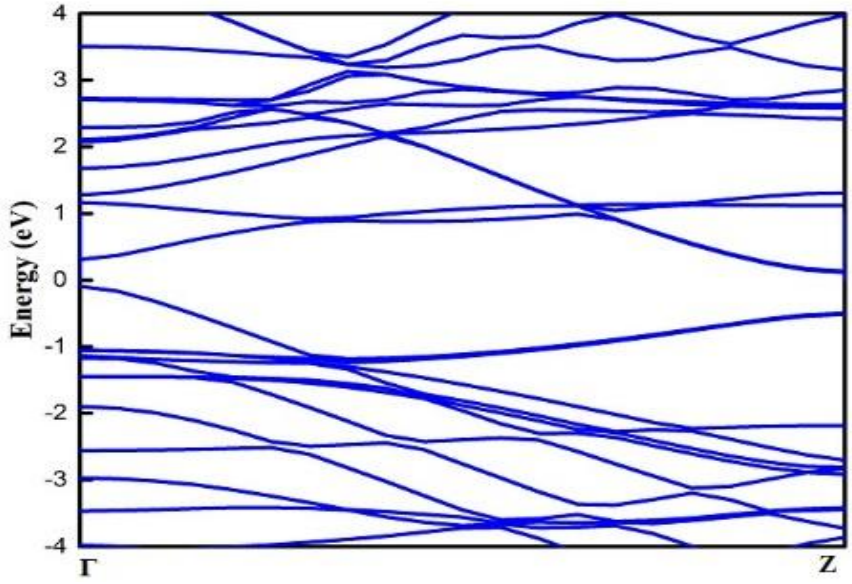

Figure 4.18 Band structure of double edge Mn terminated AGNR (N_a=9)

Similar Results have been found for the one edge Cr-terminated AGNRs in simulations, where again 3m+2 (N_a=5) family of ribbon have minimum band gap of 0.138 eV as compared to 0.233 eV of 3m+1 family (N_a=4) and 0.208 eV of 3m family (N_a=6) whereas in next three configuration (7 to 9) some members (N_a =8) are metallic. It can be seen from the results that Cr induce enhanced metallicity in the ribbon than Mn. This is further corroborated by the predictions in the simulations that shows metallic behaviour in two edge termination in N_a=5 and N_a=6 ribbons, where N_a=4 have a band gap of 0.5 eV.

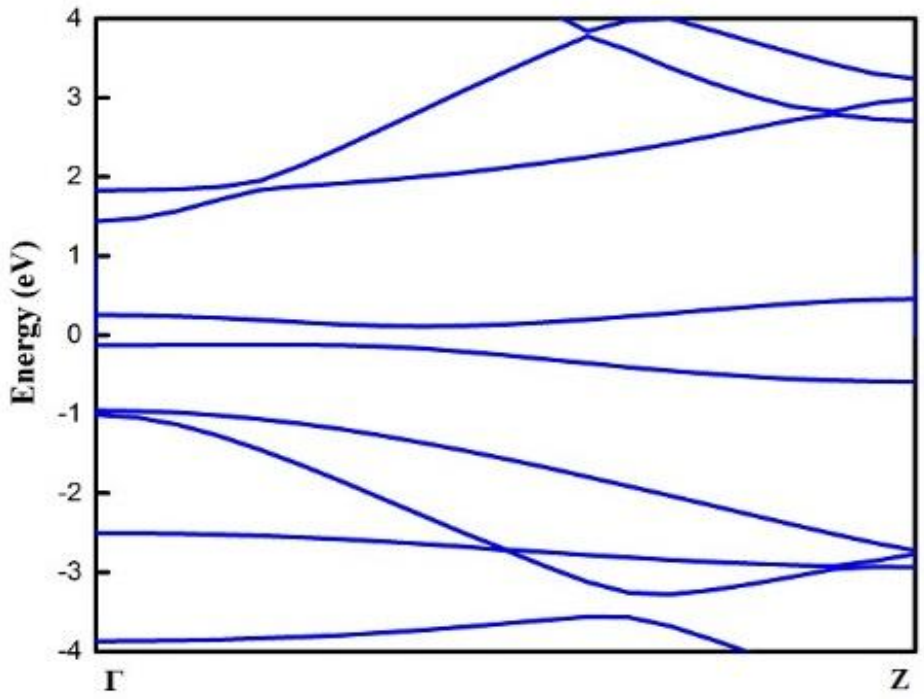

Figure 4.19 Band structure of single edge Cr terminated AGNR (N_a =4)

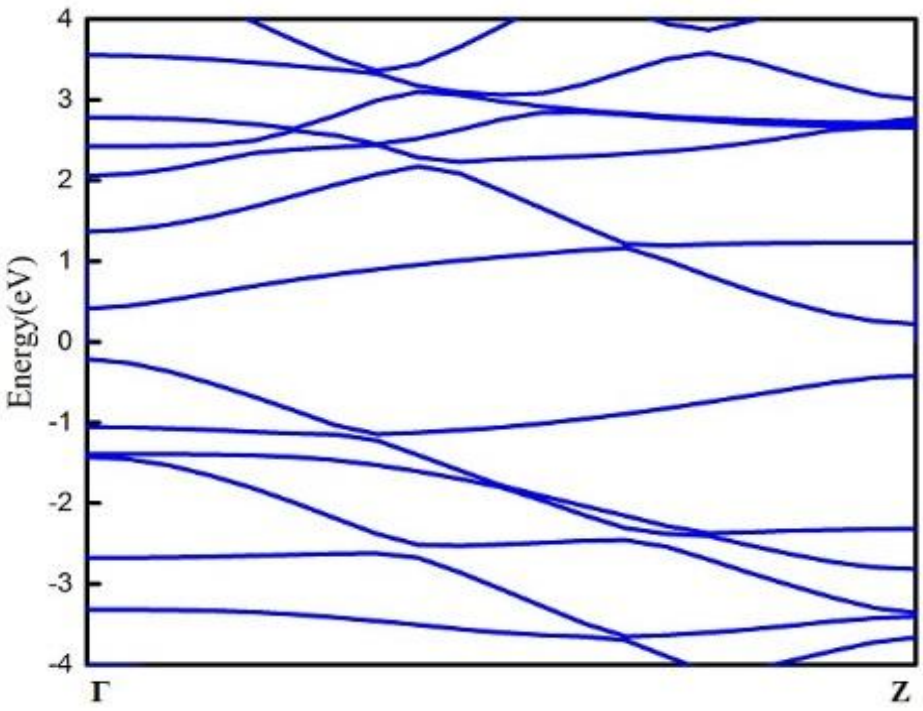

Figure 4.20 Band structure of double edge Cr terminated AGNR (N_a = 4)

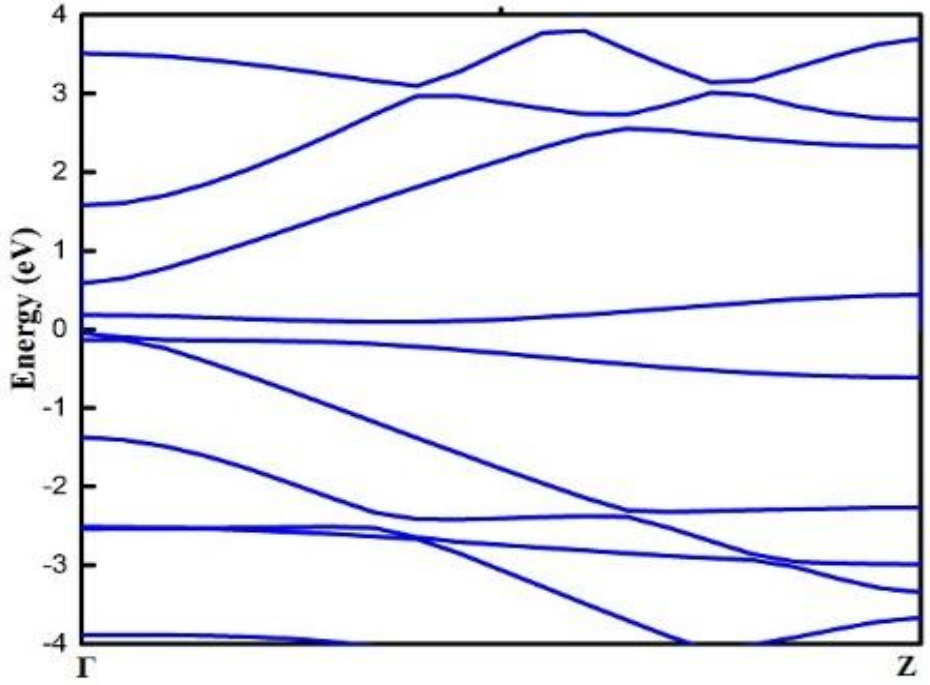

Figure 4.21 Band structure of single edge Cr terminated AGNR (N_a = 5)

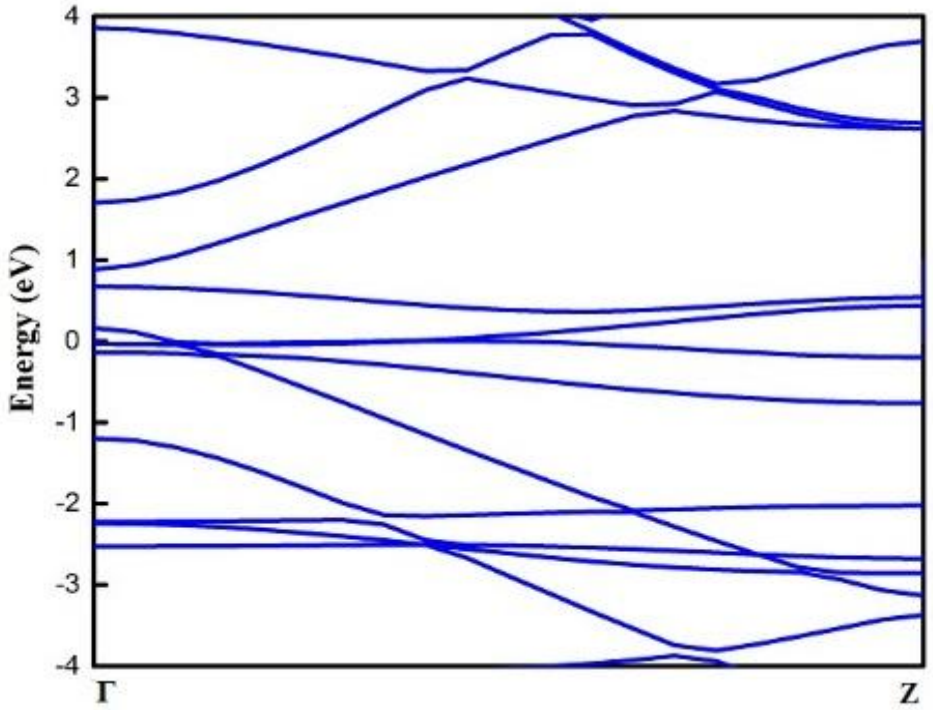

Figure 4.22 Band structure of double edge Cr terminated AGNR (N_a = 5)

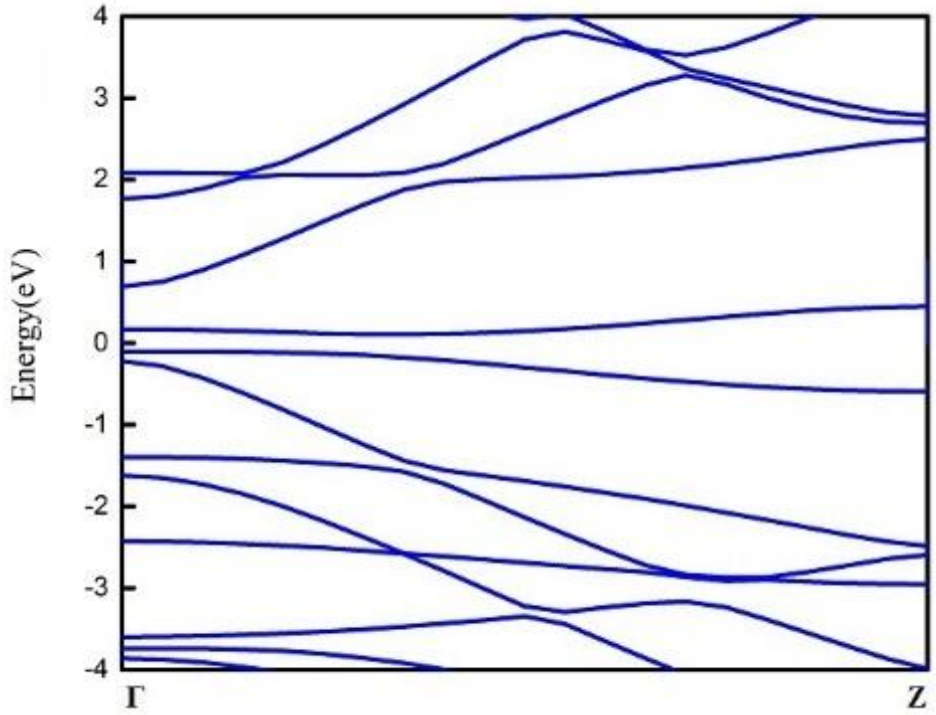

Figure 4.23 Band structure of single edge Cr terminated AGNR (N_a= 6)

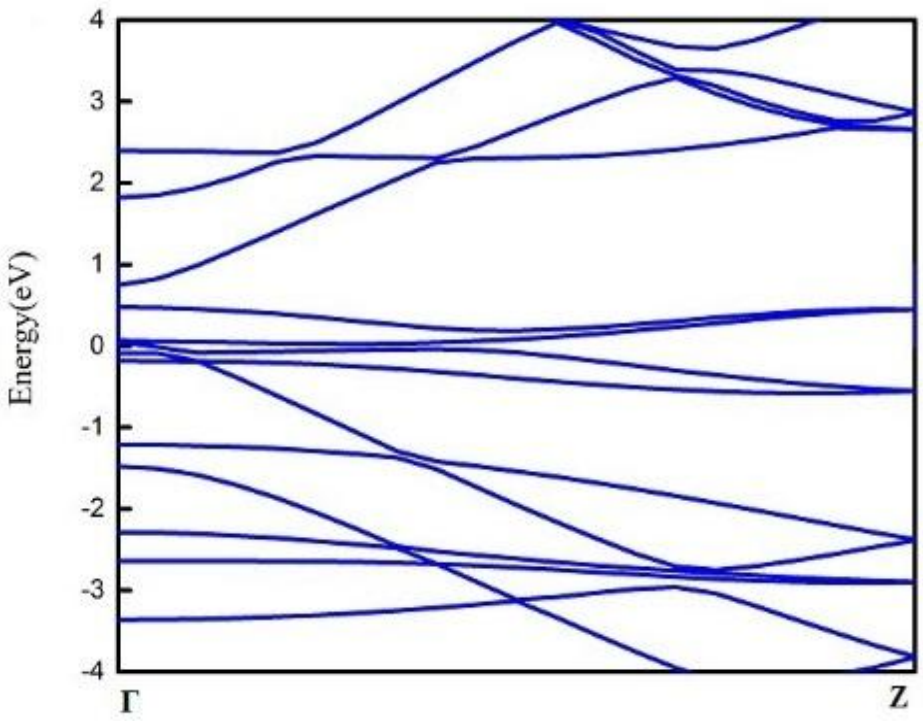

Figure 4.24 Band structure of double edge Cr terminated AGNR (N_a = 6)

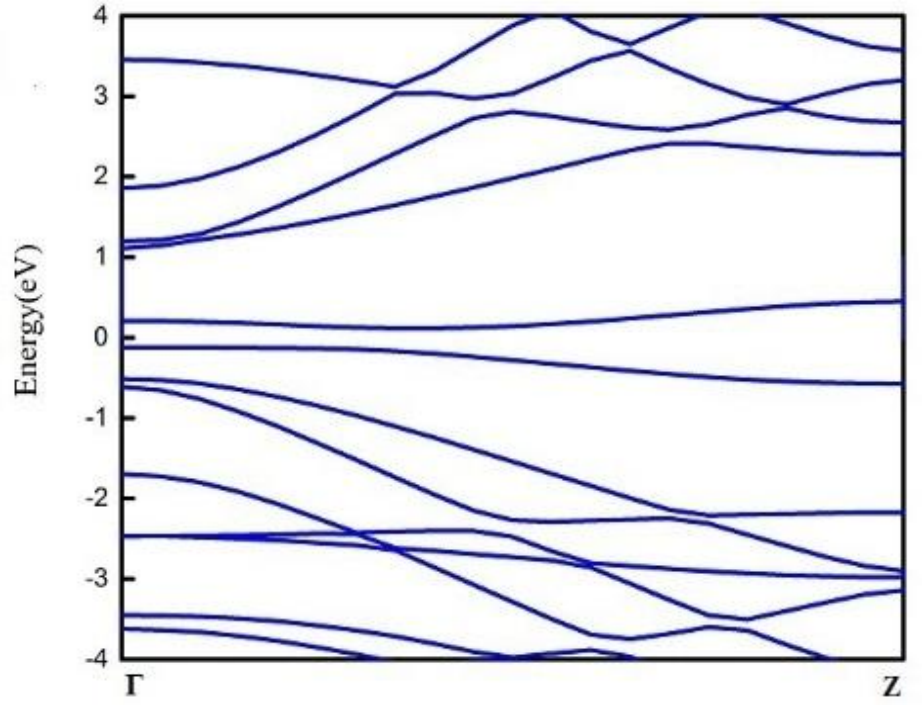

Figure 4.25 Band structure of single edge Cr terminated AGNR (N_a = 7)

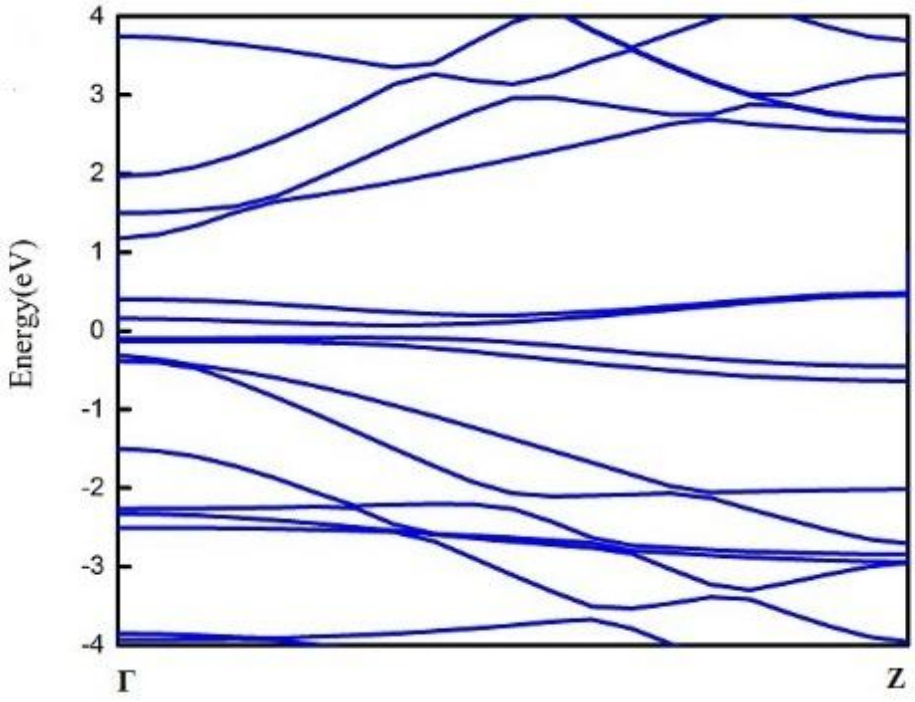

Figure 4.26 Band structure of double edge Cr terminated AGNR (width = 7)

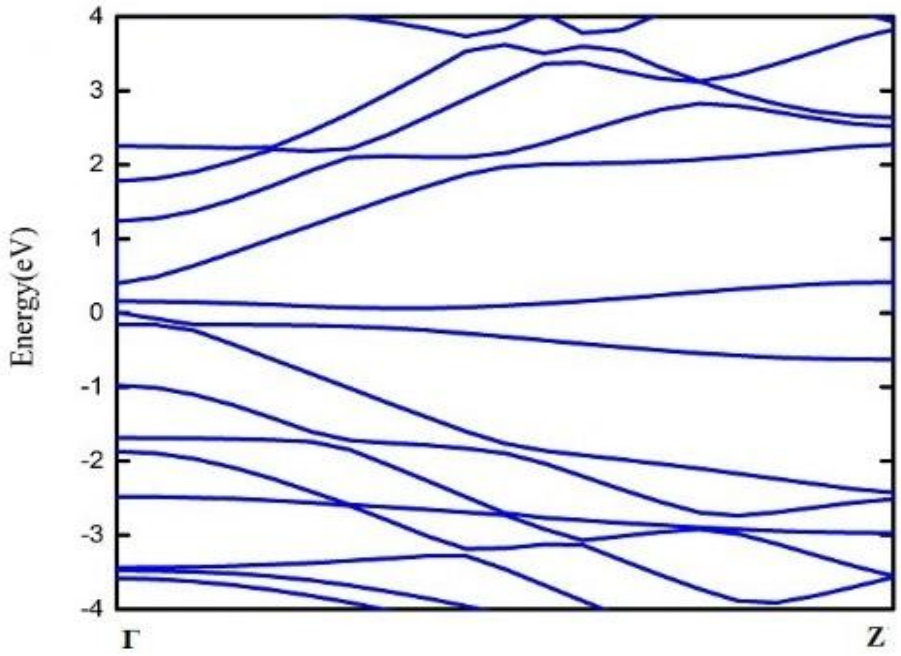

Figure 4.27 Band structure of single edge Cr terminated AGNR (N_a = 8)

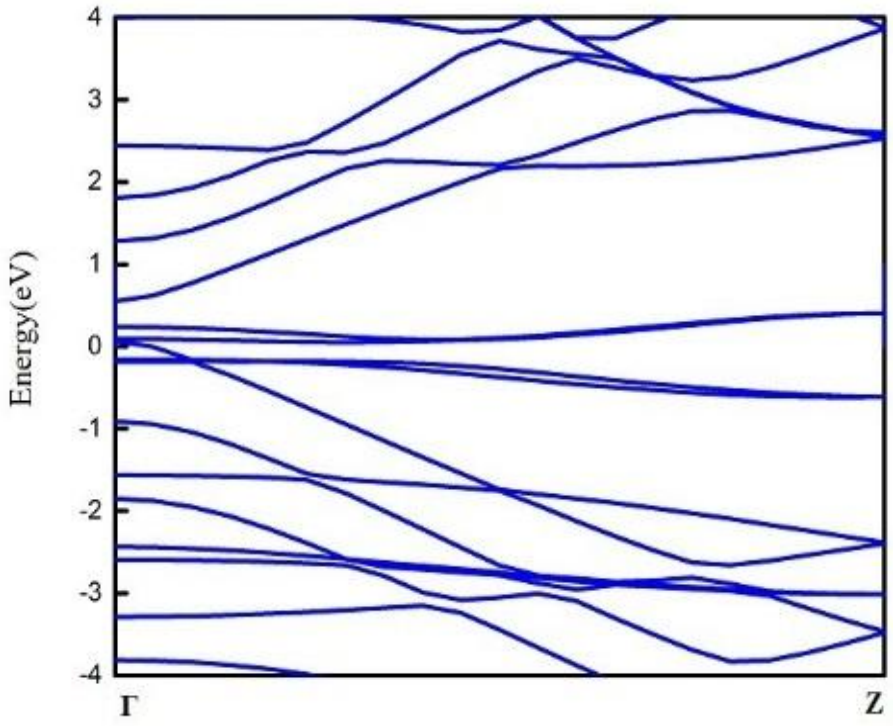

Figure 4.28 Band structure of double edge Cr terminated AGNR (N_a = 8)

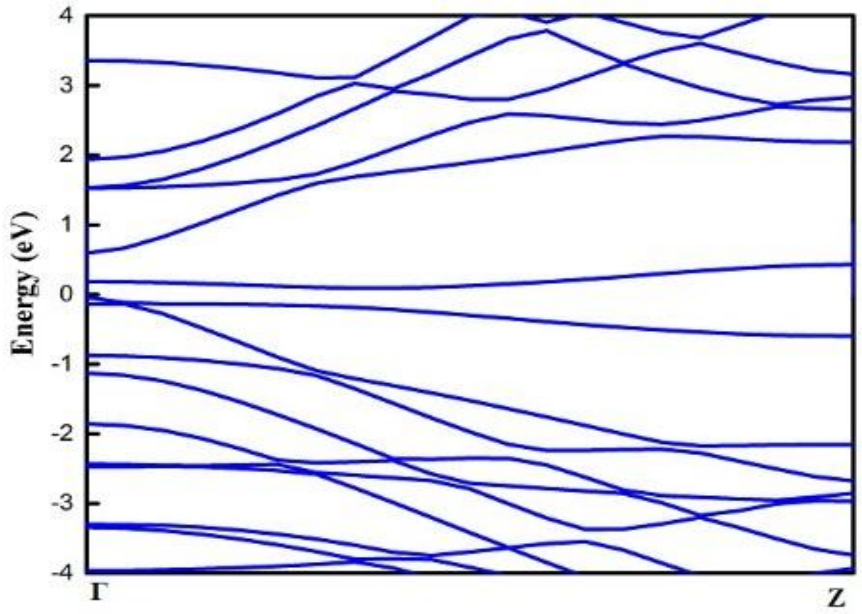

Figure 4.29 Band structure of single edge Cr terminated AGNR (N_a = 9)

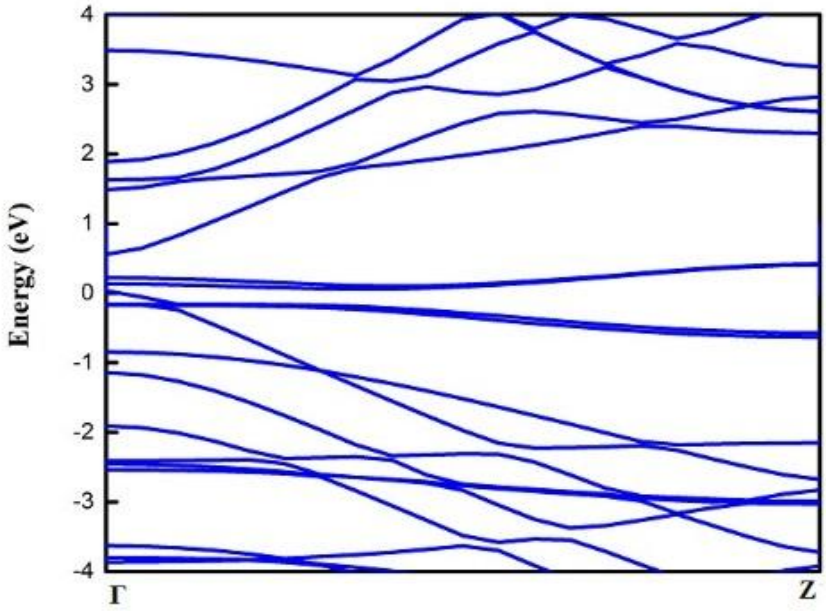

Figure 4.30 Band structure of double edge Cr terminated AGNR (width = 9)

CHAPTER 5
CONCLUSION

The energy band structure and binding energies of Mn terminated and Cr terminated AGNRs have been investigated using first principle calculations based on density functional theory. All the considered configurations are inherently stable as shown by binding energy calculations .Termination with Mn/Cr has converted the wide band gap AGNRs in narrow band gap AGNRs restricting the band gap below 1 eV in all the configurations and pushing them towards metallicity. This all can be explained by the strong hybridization between the C-2p and Mn /Cr -3d, 4s electrons in the conduction band and subsequently due to charge transfer between the metals and the edge carbon atoms. The bond length between the Mn and carbon atom is found to be 2.11 Å whereas the bond length between the edge carbon atoms has changed from 1.42 Å to 1.39 Å. It can be seen that the Mn and Cr terminated AGNRs provide wide range of possible electronic structure .Present study leads to a practical way of engineering the electronic properties of AGNR for various technical applications.

REFERENCES

1. **Novoselov, Kostya S., Andre K. Geim, S. V. Morozov, D. Jiang, Y_ Zhang, SV and Dubonos, I. V. Grigorieva, and A. A. Firsov.** 2004, science, Vol. 306, p. 666.

2. **Geim AK, Novoselov KS.** 2007, Nat Mat, Vol. 6, p. 91.

3. **Balandin AA, Ghosh S, Bao W, Calizo I, Teweldebrhan D, Miao.** 2008, Nano Lett , Vol. 8, p. 7.

4. **Balandin, Alexander A.** 2011, Nature materials, Vol. 10, p. 569.

5. **Neto, A. H. C. and Novoselov, K.** 2011, Rep. Prog. Phys., Vol. 74, p. 82.

6. **Peng, Xihong, Fu Tang, and Andrew Copple.** 2012, Journal of Physics: Condensed Matter, Vol. 24, p. 075.

7. **Jaiswal, Neeraj K., and Pankaj Srivastava.** 2011, Physica E: Low-dimensional Systems and Nanostructures, Vol. 44, p. 75.

8. **Son, Y.-W., Cohen, M. L. and Louie, S. G.** 2006, Phys. Rev. Lett., Vol. 97, p. 216803.

9. **Nakada, K., et al.** 1996, Phys. Rev. B , Vol. 54, p. 17954.

10. **Suenaga, K. and Koshino, M.** 2010, Nature, Vol. 468, p. 1088.

11. **Ma, Fei, Zhankui Guo, Kewei Xu, and Paul K. Chu.** 2012, Solid State Communications , Vol. 152, p. 1089.

12. **Lu, Y. H., R. Q. Wu, L. Shen, M. Yang, Z. D. Sha, Y. Q. Cai, P. M. He, and Y. P. Feng.** 2009, Applied Physics Letters, Vol. 94, p. 122111.

13. **Jaiswal, N. K., & Srivastava, P.** 2011, Solid State Communications,, Vol. 151, p. 1490.

14. **Rigo, V. A., Martins, T. B., da Silva, A. J., Fazzio, A., & Miwa, R. H.** 2009, Physical Review B, Vol. 79, p. 075435.

15. **Cervantes-Sodi, F., Csanyi, G., Piscanec, S., & Ferrari, A. C.** 2008, Physical Review B,, Vol. 77, p. 165427.

16. **Xu, N., Huang, B., Li, J., & Wang, B.** 2015, Solid State Communications, Vol. 202, p. 39.

17. **Sutter, Peter W., Jan-Ingo Flege, and Eli A. Sutter.** 2008, Nature materials, Vol. 7, p. 406.

18. **De Heer, W.A., Berger, C., Wu, X., First, P.N., Conrad, E.H., Li, X., Li, T., Sprinkle, M., Hass, J., Sadowski, M.L. and Potemski, M.,.** 2007, Solid State Communications,, Vol. 143, p. 92.

19. **Gao, Li, Jeffrey R. Guest, and Nathan P. Guisinger.** 2010, Nano letters , Vol. 10, p. 3512.

20. **Kosynkin, Dmitry V., Amanda L. Higginbotham, Alexander Sinitskii, Jay R. Lomeda, Ayrat Dimiev, B. Katherine Price, and James M. Tour.** 2009, Nature, Vol. 458, p. 872.

21. **Jiao, Liying, Li Zhang, Xinran Wang, Georgi Diankov, and Hongjie Dai.** 2009, Nature, Vol. 458, p. 877.

22. **Wu, Zhong-Shuai, Wencai Ren, Libo Gao, Bilu Liu, Jinping Zhao, and Hui-Ming Cheng.** 2010, Nano Research, Vol. 3, p. 16.

23. **Gorjizadeh, Narjes, and Yoshiyuki Kawazoe.** 2008, Materials transactions, Vol. 49, p. 2445.

24.. **Lu, Yang, and Jing Guo.** 3, 2010, Nano Research, Vol. 3, p. 189.

25. **Li, Yang, Xiaowei Jiang, Zhongfan Liu, and Zhirong Liu.** 8, 2010, Nano Research , Vol. 3, p. 545.

26.**Chakraborty, Tapash**., 2010. Graphene,. arXiv preprint arXiv:1011.0444.

27.**Geim, A.K. and Novoselov, K.S**., 2007. Nature materials, 6(3), pp.183-191.

28. **Nair, R.R., Blake, P., Grigorenko, A.N., Novoselov, K.S., Booth, T.J., Stauber, T., Peres, N.M. and Geim, A.K.,** 2008. 320(5881), pp.1308-1308

29.**Wang, F., Zhang, Y., Tian, C., Girit, C., Zettl, A., Crommie, M. and Shen, Y.R.,** 2008.. science, 320(5873), pp.206-209

30. **Lee, C., Wei, X., Kysar, J.W. and Hone, J**., 2008. science,321(5887), pp.385-388.

31.**Ni, Z.H., Yu, T., Lu, Y.H., Wang, Y.Y., Feng, Y.P. and Shen, Z.X.,** 2008. ACS nano, 2(11), pp.2301-2305.

32.**Balandin, A.A., Ghosh, S., Bao, W., Calizo, I., Teweldebrhan, D., Miao, F. and Lau, C.N**., 2008. Nano letters, 8(3), pp.902-907.

33.**Edwards, R.S. and Coleman, K.S**., 2013. Nanoscale, 5(1), pp.38-51.

34.**Su, C.Y., Lu, A.Y., Xu, Y., Chen, F.R., Khlobystov, A.N. and Li, L.J.,** 2011 ACS nano, 5(3), pp.2332-2339.

35.**Wang, G., Shen, X., Wang, B., Yao, J. and Park, J**., 2009., 47(5), pp.1359-1364.

36.**Huang, H., Xia, Y., Tao, X., Du, J., Fang, J., Gan, Y. and Zhang, W**., 2012 Journal of Materials Chemistry, 22(21), pp.10452-10456.

37.**Emtsev, K.V., Bostwick, A., Horn, K., Jobst, J., Kellogg, G.L., Ley, L., McChesney, J.L., Ohta, T., Reshanov, S.A., Röhrl, J. and Rotenberg, E**., 2009.. Nature materials, 8(3), pp.203-207.

38. **Riedl, C., Coletti, C., Iwasaki, T., Zakharov, A.A. and Starke, U.,** 2009. Physical review letters, 103(24), p.246804.

39.**Woodworth, A.A. and Stinespring, C.D**., 2010. Carbon, 48(7), pp.1999-2003.

40. **Kohn, Walter, and Lu Jeu Sham.** 4A, 1965, Physical review, Vol. 140, p. A1133.

41. **[Online] www.quantumwise.com.**

42**. Brandbyge, Mads, José-Luis Mozos, Pablo Ordejón, Jeremy Taylor, and Kurt Stokbro.** 16, 2002, Physical Review , Vol. B 65, p. 165401.

43. **Taylor, Jeremy, Hong Guo, and Jian Wang.** 24, 2001, Physical Review B, Vol. 63, p. 245407.

44**.Perdew, John P., and Alex Zunger.** 10, 1981, Physical Review B, Vol. 23, p. 5048.

45**. Kan, Er-Jun, H. J. Xiang, Jinlong Yang, and J. G. Hou.** 16, 2007, The Journal of chemical physics , Vol. 127, p. 164706